

CONFIDENTIAL

Copy 6
RM A52F18

NACA RM A52F18

SEP 24 1952



RESEARCH MEMORANDUM

THE LONGITUDINAL CHARACTERISTICS AT MACH NUMBERS UP TO 0.92
OF A CAMBERED AND TWISTED WING HAVING 40° OF
SWEEPBACK AND AN ASPECT RATIO OF 10

By George G. Edwards, Bruce E. Tinling,
and Arthur C. Ackerman

Ames Aeronautical Laboratory
Moffett Field, Calif.

~~CLASSIFICATION CANCELLED~~

Authority naca R 73094 Date 9/15/52

By MDA 10/17/52 See _____

CLASSIFIED DOCUMENT

This material contains information affecting the National Defense of the United States within the meaning of the espionage laws, Title 18, U.S.C., Secs. 793 and 794, the transmission or revelation of which in any manner to an unauthorized person is prohibited by law.

NATIONAL ADVISORY COMMITTEE FOR AERONAUTICS

WASHINGTON

September 15, 1952

CONFIDENTIAL

NACA LIBRARY
Moffett Field, Calif.



NATIONAL ADVISORY COMMITTEE FOR AERONAUTICS

RESEARCH MEMORANDUM

THE LONGITUDINAL CHARACTERISTICS AT MACH NUMBERS UP TO 0.92
OF A CAMBERED AND TWISTED WING HAVING 40° OF
SWEEPBACK AND AN ASPECT RATIO OF 10

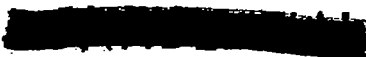
By George G. Edwards, Bruce E. Tinling,
and Arthur C. Ackerman

SUMMARY

A swept-back wing, in combination with a fuselage, of a type considered suitable for long-range, high-speed airplanes, has been investigated in the Ames 12-foot pressure wind tunnel. The wing had 40° of sweepback, an aspect ratio of 10, a taper ratio of 0.4, and 5° of wash-out at the tip. The wing thickness distribution in sections normal to the reference sweep line was the NACA 4-digit series and varied in thickness ratio from 14 percent at the root to 11 percent at the tip. These sections were cambered for a design lift coefficient of 0.40. The investigation included tests of the wing alone, the wing-fuselage combination, and the effects of fences.

Tests were conducted to measure the lift, drag, and pitching moments on a semispan model at Reynolds numbers from 2,000,000 to 8,000,000 at low Mach numbers, and at Mach numbers from 0.25 to 0.92 at a Reynolds number of 2,000,000. The boundary-layer flow on the upper surface of the wing was studied with tufts.

For Mach numbers up to 0.83, lift-drag ratios of at least 35 for the wing alone, and of at least 23 for the wing-fuselage combination were attained at lift coefficients of the order of 0.4 to 0.5. Instability of the wing developed at lift coefficients considerably below the maximum lift of the wing. However, it was found that fences on the upper surface of the wing were effective in improving the longitudinal stability of the wing at all Mach numbers and in increasing the maximum lift coefficient at low Mach numbers. It is believed that the effectiveness of these fences was at least partly attributable to the absence of leading-edge-type separation as a result of the use of camber, twist, and adequate leading-edge radii. The addition of fences increased the lift-drag



ratios at the higher lift coefficients but had little or no effect on the minimum drag or the Mach number for drag divergence.

In addition to the experimental results, this report contains a discussion of the factors considered in the selection of the geometric properties of the wing and fuselage. Estimates of the magnitudes of a number of the important aerodynamic parameters by use of available theoretical methods were in good agreement with the experimental results.

INTRODUCTION

Military and commercial requirements for higher cruising speeds and altitudes in long-range airplanes have emphasized the need for extending research concerning swept-back wings to include those of large aspect ratio. The design of such wings brings into sharp focus all the conflicting requirements for strength, stiffness, and wing weight on the one hand, and for aerodynamic efficiency on the other. Furthermore, the research data available concerning swept-back wings of moderate aspect ratio indicate that a major problem in the aerodynamic design of high aspect ratio wings is likely to be the attainment of satisfactory longitudinal stability characteristics. From a practical viewpoint all these factors must be considered in relation to the airplane performance required.

The present research was undertaken to investigate in the Ames 12-foot pressure wind tunnel a wing and a fuselage satisfying the assumed requirements of a long-range, high-speed airplane. The selection of the geometric characteristics of the wing was guided by the results of past experimental research and by calculations of the aerodynamic characteristics of the wing according to available theoretical methods.

The experimental data presented include lift, drag, and pitching-moment data for the wing alone, the fuselage alone, and the wing-fuselage combination. Included also are data which show the effects of several fence arrangements on the wing, as well as tuft photographs indicating the boundary-layer flow on the upper surface of the wing. The tests covered a range of Mach numbers up to 0.92 at a constant Reynolds number of 2,000,000, and a range of Reynolds numbers up to 8,000,000 at low Mach numbers.

NOTATION

A aspect ratio $\left(\frac{b^2}{2S} \right)$

- C_D drag coefficient $\left(\frac{\text{drag}}{qS} \right)$
- $C_{D_{\text{min}}}$ minimum profile drag coefficient assuming elliptical span load distribution $\left(\text{minimum value of } C_D - \frac{C_L^2}{\pi A} \right)$
- C_L lift coefficient $\left(\frac{\text{lift}}{qS} \right)$
- C_m pitching-moment coefficient about the quarter point of the wing mean aerodynamic chord $\left(\frac{\text{pitching moment}}{qS\bar{c}} \right)$
(See fig. 1(a).)
- C_{m_0} pitching-moment coefficient for zero lift
- c local wing chord parallel to the plane of symmetry
- C_{av} average wing chord $\left(\frac{2S}{b} \right)$
- c' wing chord perpendicular to the reference sweep line
- \bar{c} mean aerodynamic chord $\left(\frac{\int_0^{b/2} c^2 dy}{\int_0^{b/2} c dy} \right)$
- c_l section lift coefficient
- c_{l_i} design section lift coefficient
- $\frac{L}{D}$ lift-drag ratio
- M free-stream Mach number
- q free-stream dynamic pressure
- R Reynolds number based on the mean aerodynamic chord
- S area of semispan wing
- t maximum thickness of section
- y lateral distance from the plane of symmetry

S	area of semispan wing
t	maximum thickness of section
y	lateral distance from the plane of symmetry
α	angle of attack of the root chord at the plane of symmetry
ϕ	angle of twist (positive for washin) measured in planes parallel to the plane of symmetry
$\Delta\phi$	incremental twist due to wing bending
η	fraction of semispan $\left(\frac{y}{b/2}\right)$
Λ	angle of sweepback of the line through the quarter-chord points of the reference sections

DESIGN CONSIDERATIONS

The selection of the geometric properties of the wing and fuselage were based on some of the requirements of an assumed airplane capable of cruising efficiently at 550 miles per hour at an altitude of 40,000 feet ($M = 0.83$) with wing loadings of the order of 75 to 100 pounds per square foot ($C_L = 0.4$ to 0.5). The following paragraphs outline some of the factors considered in arriving at the wing-fuselage combination investigated and include estimates of a number of the important aerodynamic parameters. The latter are included for the purpose of correlating them with the experimental results later in this report. The procedure used was not a direct one because the various design variables obviously have interrelated effects on the aerodynamics of the wing. Furthermore, the effect of variations in some of the factors governing the selection of the wing geometry cannot be ascertained by direct computational methods but must be estimated on the basis of past experimental research.

Wing

Preliminary analysis and reference to past research results (see references 1, 2, and 3 for examples) suggested the type of wing required. For the attainment of best range characteristics, the required aspect ratio, considering aerodynamic aspects against those of wing weight and structural rigidity, appeared to be between 8 and 12. It was estimated

that the wing would require more than 35° sweepback, but probably less than 45° to attain a satisfactory drag-divergence Mach number with wing sections of sufficient thickness to meet strength and stiffness requirements. To avoid doubly curved surfaces, in the interest of manufacturing simplicity, elements connecting equal percent-chord points were to be linear. This requirement, in effect, fixed the spanwise variation of both thickness ratio and twist, once the total twist and the thickness ratios at the root and at the tip had been chosen.

Good longitudinal stability characteristics were considered of prime importance. On a high-aspect-ratio wing, loss of longitudinal stability at high lift coefficients is most likely to originate from decreases of lift-curve slope on the outer sections prior to any similar decreases on the inner sections. Attention was therefore directed toward means of preventing abrupt changes in the lift-curve slopes and premature stalling of the outer sections, such as might occur as a result of laminar separation near the leading edge. In the absence of leading-edge separation, the stall occurs from turbulent separation which progresses gradually forward from the trailing edge with increasing angle of attack. The accompanying changes in lift and pitching moment would therefore be expected to be gradual and the spanwise flow of the boundary-layer air to be confined to the region well behind the leading edge.

In reference 4, it has been shown that the stall could be changed from the leading-edge type to the trailing-edge type on the NACA 631-012 section by increasing the leading-edge radius and providing a small amount of camber near the leading edge. The effect of a similar modification on a 35° swept-back wing having NACA 64A010 sections (reference 5) was to increase the lift coefficient for violent longitudinal instability from 0.80 to 1.18 at a Reynolds number of 11,000,000. It is clear that such modifications to NACA 6-series sections with thickness ratios of at least 0.10 are an effective means of avoiding leading-edge separation. In considering such modified sections for the present wing, however, it was realized that these leading-edge modifications could not be employed on NACA 6-series sections without sacrificing the low-drag qualities of these sections. Therefore, sections having the NACA 4-digit thickness distribution and thickness ratios larger than 0.10 were chosen for the present wing since they have leading-edge radii¹ comparable to those which were found to be satisfactory in the previously cited investigations (references 4 and 5). Camber near the leading edge was not introduced because of lack of specific evidence that it was necessary in order to avoid leading-edge separation on the NACA 4-digit sections.

¹The leading-edge radius of the NACA 0012 section is 1.580-percent chord compared to 0.994-percent chord for the NACA 64₁A012 section.

In selecting thickness ratios for the wing sections, consideration was given to varying the thickness ratio from the root to the tip. Unpublished data available at the time this wing was designed indicated that the thickness ratios of the root sections could be increased relative to the outer sections without reducing the drag-divergence Mach number. The explanation of this appears to lie in the more uniform chordwise pressure distribution near the root (and therefore lower maximum local velocities) as compared to those of the outer sections of a swept-back wing. (See, e.g., reference 6.) In view of the structural advantage of a thicker root section, the thickness ratios normal to the reference sweep line were chosen to be 14-percent chord at the wing root and 11-percent chord at the tip. The variation of thickness ratios between the root and the tip was taken to be that which resulted in linear elements connecting points at equal percent chord at all sections. (See fig. 1(b).) It is believed that a more nearly optimum spanwise distribution of thickness ratio in regard to both structural efficiency and drag is one in which the thickness ratio decreases most rapidly in the region extending from the wing root to about one-third of the semi-span, with a gradual reduction occurring between this point and the wing tip.

The cruise conditions assumed require wing lift coefficients between 0.4 and 0.5, which correspond, according to the principles of simple sweep theory, to lift coefficients of approximately 0.8 for sections normal to the reference sweep line. Experimental results presented in reference 7 demonstrate that in this lift coefficient range camber will improve the lift-drag ratio of airfoil sections, provided the critical Mach number is not exceeded. Furthermore, the results presented in reference 8 indicate that a moderate amount of camber applied to NACA 4-digit sections improves the drag-divergence Mach number at moderate to high lift coefficients. However, from the results of investigations of wings of finite span (references 2 and 3) it was deduced that if the sections were cambered to develop section lift coefficients of the order of 0.8, it would entail a reduction in the drag-divergence Mach number, excessive turbulent separation on the upper surface, and high minimum drag. Consequently, the sections were cambered for an ideal lift coefficient of 0.4. At the cruise condition assumed, therefore, about half the section lift coefficient results from the basic loading due to camber and the remainder results from additional loading. In selecting the chordwise distribution of camber it was noted that while the $a = 0.4$ mean line provides lower pitching-moment coefficients at zero lift than the camber line for uniform loading ($a = 1.0$), the latter provides somewhat better lift and drag characteristics at high Mach numbers (reference 7). The compromise camber line selected was the $a = 0.8$ (modified) mean line (reference 9). Although there are reasons for suspecting that wing efficiency can be improved by varying the camber along the span, the same camber was used for all sections

(normal to the reference sweep line) in order to maintain standard sections at all stations and to avoid doubly curved surfaces.

The required sweepback to provide a drag-divergence Mach number equal to or greater than 0.83 was estimated to be 40° with the wing sections chosen. While a larger amount of sweepback could have been used to attain a higher drag-divergence Mach number, it would make the attainment of satisfactory longitudinal stability characteristics more difficult.

A ratio of tip chord to root chord of 0.40 was chosen as a compromise between the large tip chord desired to prevent excessive section lift coefficients at the tip and the large root chord desired for greater structural rigidity and lower wing weight.

An aspect ratio of 10 was chosen on the basis that the wing with this aspect ratio, 40° of sweepback, a taper ratio of 0.40, and the wing-root thickness ratio previously selected fitted the strength and stiffness criterion that the ratio of wing panel length $\left(\frac{b/2}{\cos \Lambda}\right)$ to the maximum thickness at the root be approximately 40. Wings having a value of this ratio of 50 are sometimes considered structurally feasible, but the more conservative value of 40 was used in order to reduce wing weight and aeroelastic effects such as wing flutter and adverse control characteristics. The wing plan form is shown in figure 1(a).

Twist (washout of the outer sections) provided a means of reducing the loading on the outer wing sections to alleviate the tendency toward longitudinal instability and, at the same time, provided a means of adjusting the spanwise distribution of load to increase span efficiency. Since this form of twist also produced a positive increment of pitching moment at zero lift, it was a means of canceling the negative pitching moment at zero lift resulting from the wing camber. The twist was introduced by rotating the streamwise sections about the leading edge while maintaining the projected plan form and was distributed along the semispan so as to avoid doubly curved surfaces (i.e., the trailing edge was a straight line). With this type of twist distribution, elliptical span load distribution could be only approximated. The spanwise distribution of load was calculated by the Weissinger method, using the procedures outlined in reference 10, for both the untwisted wing and the wing with various amounts of twist. It was found that a twist distribution as shown in figure 1(b), with 5° washout at the tip, provided nearly elliptical span load distribution and reduced the pitching moment at zero lift of the wing. Because the wing was to be mounted high on the fuselage, it was anticipated that the moment contribution of the fuselage would be negative, suggesting that the twist should be increased. However, additional wing twist was not introduced to

compensate for the fuselage pitching moment because it would have increased the possibility of lower-surface separation near the tip at low lift coefficients and caused the span load distribution to depart further from the ideal elliptical loading. The calculated span load distributions at a lift coefficient of 0.40 for the cambered wing with the twist shown in figure 1(b) are shown in figure 2 for Mach numbers of 0 and 0.83. Also shown for comparison are the calculated span load distribution for the wing without twist and an elliptical span load distribution. The calculated pitching-moment coefficient due to twist (reference 10) was 0.063. Addition of this pitching-moment coefficient to that calculated by application of simple sweep theory to the section zero-lift pitching-moment coefficient yielded a resultant zero-lift pitching-moment coefficient of 0.012. The calculated angle of attack for zero lift was -1° .

Fuselage

For the purposes of these model tests, a fuselage consisting of a cylindrical midsection with simple fairings fore and aft was used (coordinates listed in table I). The fuselage, which had a fineness ratio of 12.6, was located with respect to the wing as shown in figure 1(a), so that the upper surface of the wing was tangent to the top of the fuselage at the plane of symmetry. The high wing position was chosen in preference to a lower position to provide for the possibility of using either wing-mounted propellers or strut-mounted jet pods and to permit use of a lower horizontal-tail position with respect to the wing. Estimates of the angle of zero lift and lift-curve slope of the wing (reference 10) indicated that the incidence of the wing root relative to the fuselage center line should be about 3° for minimum fuselage drag at a lift coefficient of 0.4.

MODEL

The semispan model tested simulated a wing having an aspect ratio of 10, a taper ratio of 0.4, and 40° of sweepback. (See fig. 1(a).) The reference sweep line was the line joining the quarter-chord points of the sections inclined 40° to the plane of symmetry (26.65 percent of the streamwise chord). The thicknesses of sections perpendicular to the reference sweep line varied from 14 percent of the chord at the root to 11 percent of the chord at the tip. The tip was washed out 5° . The variations of twist and thickness ratio along the semispan are shown in figure 1(b). The sections perpendicular to the reference sweep line were formed by combining an NACA 4-digit thickness distribution with an $a = 0.8$ modified mean line (reference 9) having an ideal lift

coefficient of 0.40. The coordinates of the NACA 4-digit thickness distributions and the method of combining the thickness distribution with the mean line are given in reference 11.

The wing was constructed of steel and was equipped with flush orifices for the measurement of surface pressures. No flow was permitted through these orifices during the present tests.

The fuselage, which had the coordinates listed in table I, was constructed of mahogany bolted to a heavy steel structural member. The fuselage was located with respect to the wing as shown in figure 1(a).

The model was tested with several combinations of boundary-layer fences on the upper surface of the wing. Sketches of the two types of fences used and their locations on the wing are shown in figure 3. Photographs showing the model in the wind tunnel and details of the fence installation are presented in figure 4.

TESTS

Tests were conducted of the wing alone, the wing-fuselage combination, and the fuselage alone. The lift, drag, and pitching-moment coefficients were measured at Reynolds numbers from 2,000,000 to 8,000,000 at low Mach numbers and at Mach numbers from 0.25 to 0.92 at a Reynolds number of 2,000,000. Tuft studies with and without various fence combinations were made at several Mach numbers. Exploratory tests of this nature were conducted at a Reynolds number of 8,000,000 and a Mach number of 0.25, and at Mach numbers of 0.25, 0.80, and 0.90 at a Reynolds number of 2,000,000. A series of force tests covering the complete range of Reynolds numbers and Mach numbers was then conducted on the wing-fuselage combination using the most satisfactory of the fence configurations.

CORRECTIONS TO DATA

The data have been corrected for constriction effects due to the presence of the tunnel walls, for tunnel-wall interference effects originating from lift on the model, and for the drag tares caused by aerodynamic forces on the exposed portion of the turntable on which the model was mounted.

The dynamic pressure was corrected for constriction effects due to the presence of the tunnel walls by the methods of reference 12. These corrections were not modified to allow for the effects of sweep. This correction and the corresponding correction to the Mach number are listed in the following table:

Corrected Mach number	Wing		Fuselage		Wing and fuselage	
	Uncor- rected Mach number	$\frac{q_{corrected}}{q_{uncorrected}}$	Uncor- rected Mach number	$\frac{q_{corrected}}{q_{uncorrected}}$	Uncor- rected Mach number	$\frac{q_{corrected}}{q_{uncorrected}}$
0.165	0.165	1.001	- - -	- - -	0.165	1.003
.25	.250	1.001	0.250	1.003	.250	1.004
.60	.599	1.002	.598	1.004	.598	1.006
.70	.699	1.002	.697	1.006	.696	1.008
.80	.797	1.003	.794	1.008	.793	1.011
.83	.827	1.004	.823	1.009	.820	1.012
.86	.856	1.005	.850	1.012	.848	1.014
.88	.875	1.006	.868	1.014	.866	1.018
.90	.894	1.007	.886	1.017	.883	1.022
.92	.912	1.008	.903	1.020	.898	1.026

Corrections for the effects of tunnel-wall interference originating from lift on the model were calculated by the method of reference 13. The corrections to the angle of attack and to the drag coefficient showed insignificant variations with Mach number. The corrections added to the data were as follows:

$$\Delta\alpha = 0.377 C_L$$

$$\Delta C_D = 0.0059 C_L^2$$

The correction to the pitching-moment coefficient had a significant variation with Mach number. The following correction was added to the measured pitching-moment coefficients:

$$\Delta C_m = K C_L$$

where K is given in the following table:

M	K
0.165	0.0030
.25	.0032
.60	.0048
.70	.0056
.80	.0069
.83	.0073
.86	.0078
.88	.0082
.90	.0087
.92	.0091

Since the turntable upon which the model was mounted was directly connected to the balance system, a tare correction to the drag was necessary. The magnitude of this correction for the wing alone was determined from tests with the model removed from the wind tunnel. The correction to the data for the wing-fuselage combination and the fuselage alone was obtained by multiplying the correction for the wing alone by the fraction of the area of the turntable still exposed to the air stream after installation of the fuselage. The following tare corrections were subtracted from the measured drag coefficients:

Mach number	Reynolds number	Wing	Wing and fuselage or fuselage alone
0.165	8,000,000	0.0033	0.0025
.25	8,000,000	.0033	.0024
.25	6,000,000	.0033	.0025
.25	4,000,000	.0033	.0025
.25	2,000,000	.0034	.0025
.60	2,000,000	.0034	.0025
.70	2,000,000	.0035	.0026
.80	2,000,000	.0038	.0028
.83	2,000,000	.0039	.0029
.86	2,000,000	.0040	.0030
.88	2,000,000	.0042	.0031
.90	2,000,000	.0043	.0032
.92	2,000,000	.0045	.0034

No attempt has been made to evaluate tares due to interference between the model and the turntable or to compensate for the tunnel-floor boundary layer which, at the turntable, had a displacement thickness of one-half inch.

To establish the magnitude of possible aeroelastic effects, a static load test of the model wing was made to determine the twist due to bending. A 1000-pound load was distributed along the span according to the theoretical distribution calculated for incompressible flow for a lift coefficient of 1.0 by the method of reference 10. The results are presented in figure 5. For convenience, the loads on the wing per unit lift coefficient for various test conditions are also presented in this figure. Calculations from these data indicate that the twist due to bending, $\Delta\phi$, at the test condition where the aerodynamic load is greatest ($M = 0.25$, $R = 8,000,000$) is about -2.2° (at the tip) per unit lift coefficient. The aerodynamic data have not been corrected for the effects of this aeroelastic distortion.

RESULTS

Results of tests of the wing alone are presented in figures 6 and 7. Figure 6 shows lift, drag, and pitching-moment data obtained at Reynolds numbers from 2,000,000 to 8,000,000 and a Mach number of 0.25, and figure 7 shows similar data obtained at Mach numbers from 0.25 to 0.92 and a Reynolds number of 2,000,000. Test results for the wing-fuselage combination covering the same range of Reynolds numbers and Mach numbers as for the wing alone are presented in figures 8 and 9, and those for the fuselage alone are presented in figure 10. The data for the wing alone are compared with those for the wing-fuselage combinations in figures 11 through 13.

Data obtained during the development of a satisfactory fence configuration for the wing-fuselage combination are presented in figures 14 through 17. Photographs of tufts on the wing to indicate the direction of the boundary-layer flow both with and without fences are presented in figure 18. The results of tests of the wing-fuselage combination with the most satisfactory fence configuration are presented in figures 19 and 20 and the lift-drag ratios are compared with those for the wing-fuselage combination without fences in figure 21.

A summary plot showing the effect of Reynolds number on the lift-drag ratios of the wing alone, the wing-fuselage combination, and the wing-fuselage combination with the most satisfactory fences is presented in figure 22. Summary plots showing the effect of Mach number on several of the aerodynamic characteristics are presented in figures 23, 24, and 25.

In some instances the data have been faired with a dotted line. This practice was followed whenever the static pressure on the tunnel

wall opposite the upper surface of the wing indicated a local Mach number greater than 1.0. Under these conditions the wind tunnel may have been partially choked.

DISCUSSION

Wing Alone

Low speed.- From the data of figure 6, it may be noted that the angle of attack and the pitching-moment coefficient for zero lift agreed closely with the design values of -1° and 0.012, respectively. Although large reductions of static longitudinal stability occurred with increasing lift coefficient in the high lift range, it is apparent from the pitching-moment curves that these changes were of a gradual nature. The stability changes, the decrease of lift-curve slope, and the abrupt drag increase were all delayed to higher lift coefficients as the Reynolds number was increased. Reference to the tuft photographs in figures 18(a) and 18(b) for the wing without fences shows that there was no leading-edge separation and that the region of spanwise flow of the boundary layer was confined to the rear portions of the wing until the outer sections stalled. The tuft photographs show clearly that increasing the Reynolds number reduced the extent of spanwise flow.

The maximum lift-drag ratio for the wing alone was approximately 35 at all Reynolds numbers and occurred at a lift coefficient of about 0.4 as shown by figure 22. An increase of Reynolds number increased the lift-drag ratio markedly at lift coefficients greater than 0.8.

High speed.- As may be noted from the data of figure 7, the angle of attack for zero lift varied only slightly from its design value of -1° throughout the range of Mach numbers from 0.25 to 0.92. The pitching-moment coefficient at zero lift, however, became slightly negative with increasing Mach number, attaining a value of -0.015 at a Mach number of 0.92.

The reduction in longitudinal stability and abrupt increase in drag occurred at lower lift coefficients as the Mach number was increased. The flow changes accompanying these stability and drag changes can be observed in the tuft photographs in figures 18(c) and 18(d). At a Mach number of 0.80 the tuft photographs indicate that the flow was rough over the midsemispan at angles of attack between 6° and 8° , corresponding to lift coefficients between 0.6 and 0.7. The tuft photographs for a Mach number of 0.90 and an angle of attack of 4.1° (fig. 18(d)) show a well-defined line of disturbed tufts extending from the wing root to about 70 percent of the semispan, probably caused by the action of a shock wave.

The drag data of figure 7(b) have been cross-plotted as a function of Mach number for constant values of lift coefficient in figure 23(a). The Mach numbers for drag divergence, defined as the Mach number where $\partial C_D / \partial M = 0.1$, measured from these data are as follows:

C_L	Mach number for drag divergence
0.2	Not attained
.3	0.89
.4	.87
.5	.83
.6	.79
.7	.73

These data show that drag divergence did not occur up to the design cruise Mach number, 0.83, at lift coefficients of 0.5 or less.

Maximum lift-drag ratios somewhat greater than the low-speed value of 35 were obtained for Mach numbers up to about 0.83, as shown in figure 24. Further increase of Mach number to 0.92 resulted in a reduction of maximum lift-drag ratio to 21. The lift coefficient for maximum lift-drag ratio was approximately 0.37 at Mach numbers less than 0.83 and decreased with further increase in Mach number.

The variation of the drag coefficient and of the lift- and pitching-moment-curve slopes for a lift coefficient near that for maximum lift-drag ratio ($C_L = 0.4$) is presented in figure 25. These data indicate that an abrupt decrease of lift-curve slope and a reduction of static longitudinal stability occurred at the Mach number for drag divergence. Although not shown, a similar correlation also exists for other values of lift coefficient.

Fuselage and Wing-Fuselage Combination

The lift, drag, and pitching-moment coefficients of the fuselage are based on the area, the mean aerodynamic chord, and the moment center of the wing, and are presented in figure 10 as functions of the angle of attack of the wing root chord, which is greater than the angle of attack of the fuselage center line by 3° .

The difference in minimum profile drag between that of the wing alone and the wing-fuselage combination (fig. 11) was approximately equal to the drag of the fuselage alone (fig. 10) as may be seen from the following table:

Mach number	Reynolds number	Minimum profile drag coefficient, $C_{D_{min}}$			
		Wing alone	Wing-fuselage combination	$\Delta C_{D_{min}}$	Fuselage alone
0.25	8,000,000	0.0058	0.0099	0.0041	0.0038
.25	2,000,000	.0059	.0097	.0038	.0042
.80	2,000,000	.0055	.0106	.0051	.0048
.90	2,000,000	.0073	.0138	.0065	.0059

The addition of the fuselage caused very little, if any, unfavorable drag interference and no change in the Mach number for drag divergence (fig. 25).

It was considered possible that favorable drag interference effects might exist which were nullified by separation on the lower surface originating from the wing-fuselage juncture. Accordingly, an attempt was made to improve the flow by means of a fillet. Although observations of tufts at Mach numbers of 0.25 and 0.60 indicated that a fillet improved the flow in and behind the wing-fuselage juncture at moderate and high lift coefficients, no significant drag reduction was indicated by force measurements with the tufts removed.

Addition of the fuselage to the wing caused a rather large reduction in the maximum lift-drag ratio, as may be seen from the data of figures 12 and 24. The maximum lift-drag ratio of the wing-fuselage combination varied from about 26 at a Mach number of 0.25 to 23 at the design cruise Mach number, 0.83. Further Mach number increase to 0.92 caused the lift-drag ratio to decrease to 14. As would be anticipated from the increase in minimum drag, the lift coefficient for maximum lift-drag ratio for the wing-fuselage combination was greater than for the wing alone. (See fig. 24.)

At a lift coefficient of 0.4, addition of the fuselage to the wing increased the lift-curve slope slightly and changed the slope of the pitching-moment curve by as much as 0.07. (See fig. 25.) The pitching-moment coefficient at zero lift was changed by about -0.04. (See fig. 11.) A comparison of the pitching-moment coefficients obtained by adding the wing-alone and fuselage-alone pitching-moment coefficients with those measured for the wing-fuselage combination is presented in figure 13. These data indicate that the change in slope caused by the addition of the fuselage was approximately that which would be anticipated from the pitching-moment characteristics of the fuselage alone. However, the change in C_{m_0} was greater than that obtained in this way, indicating that interference reduced the basic load on the inner sections of the wing.

Effect of Fences

Small fences.- The first fences investigated were designed without benefit of test data or tuft photographs for this wing. Because of the large leading-edge radius, camber, and twist, it was expected that there would be no leading-edge separation and that spanwise flow of the boundary layer would be confined to the rear portions of the wing. The fences were essentially triangular as shown in figure 3.

The effects of single and multiple fences of this type at a Mach number of 0.25 and a Reynolds number of 2,000,000 are shown in figure 14. The data show that single fences at either 50 or 75 percent of the semispan produced only small improvements in the pitching-moment characteristics. The joint effect of these fences, however, was somewhat greater than the sum of the individual effects of the fences. Addition of a third fence at 33 percent of the semispan produced a further improvement in the pitching-moment characteristics. These improvements were, in all cases, accompanied by increases in the lift-curve slope and by delays in the abrupt drag rise with lift coefficient. It is of interest to note that at a Reynolds number of 2,000,000, the effects of increasing the number of fences (fig. 14) were similar to increasing the Reynolds number (fig. 8). However, reference to figure 15(b) will show that the three small fences (denoted A, B, and C) also produced a marked improvement of the aerodynamic characteristics at a Reynolds number of 8,000,000; in fact, they made the wing-fuselage combination longitudinally stable at the stall.

The three small fences (A, B, and C) did not substantially improve the pitching-moment characteristics at Mach numbers of 0.80 and 0.90. (See figs. 15(c) and 15(d).) The tuft photographs in figures 18(c) and 18(d) show that at these Mach numbers separation, probably induced by a shock wave, occurred considerably forward of the fences.

Extended fences.- In order to interrupt the spanwise flow within the separated region at high Mach numbers, the two outer fences were replaced with three fences extending well forward of the region of separation (fig. 3). These fences were placed at 50, 70, and 85 percent of the semispan. This fence configuration (denoted A, D, E, and F in the figures) proved to be very effective in improving the pitching-moment characteristics at the higher Mach numbers as shown in figures 15(c) and 15(d), as well as at a Mach number of 0.25 as shown in figures 15(a) and 15(b). The effects of this fence arrangement on the aerodynamic characteristics of the wing alone at a Mach number of 0.165 (corresponding to a reasonable landing speed) at a Reynolds number of 8,000,000 are shown in figures 16 and 17. These data show that addition of the four fences increased the lift coefficient at which a large decrease of static

longitudinal stability occurred by about 0.4, increased the maximum lift coefficient by about 0.2, and caused a large reduction in drag due to lift at lift coefficients above 1.0. It was not possible to conduct a similar test of the wing-fuselage combination since the maximum available angle of attack with the fuselage installed was less than that for maximum lift.

Complete data for the wing-fuselage combination with these fences are given in figure 19 for a Mach number of 0.25 at several Reynolds numbers and in figure 20 for a range of Mach numbers at a constant Reynolds number of 2,000,000. It may be noted from these data that with these fences, large changes in longitudinal stability with increasing lift coefficients were eliminated up to a lift coefficient of at least 0.60 at all test Mach numbers. The addition of the fences caused only small reductions in the maximum lift-drag ratios, as may be seen from figures 21 and 24, and this in spite of the exposed flange used in mounting the fences. (See photograph of fences, fig. 4.) At large values of lift coefficient, the lift-drag ratio was improved by the fences (see fig. 21).

With reference to figure 25 (data shown are for $C_L = 0.40$), it is noted that the fences caused very little change in the Mach number for drag divergence. The fences increased the lift-curve slope and the static longitudinal stability slightly at Mach numbers up to about 0.80. With further increase in Mach number, there was an abrupt increase in stability of the wing with fences in contrast with the abrupt decrease which occurred without fences.

Remarks Concerning Spanwise Flow

The present study of the effects of fences on the aerodynamic characteristics of this wing and the tuft studies of the flow prompt some remarks regarding the influence of spanwise flow of the boundary layer.

The changes in longitudinal stability throughout the lift range of a swept-back wing of high aspect ratio result primarily from changes in the spanwise distribution of loading. As has been shown in reference 14, the spanwise flow of boundary-layer air is at least partly responsible for these changes in loading. In that investigation, a study of this phenomenon on a cambered and twisted swept-back wing revealed that, while the maximum local lift coefficients of the outer sections were equal to those calculated by application of simple sweep theory to two-dimensional data, the local maximum lift coefficients of the inner sections were considerably in excess of the predicted values as a result of boundary-layer control afforded by the outward flow of boundary-layer

air. The increased lift near the wing root in comparison with that on the outer sections caused a strong pitch-up tendency at high lift coefficients.

The data presented herein indicate that the fences increased the maximum lift coefficient of the wing and eliminated, or at least delayed to higher lift coefficients, the unstable trend of pitching moments at high lift coefficients. A question arises as to whether the fences produced the stabilizing effect through a reduction in the boundary-layer-control effect on the root sections, thereby reducing the lift on those sections. The fact that the maximum lift coefficient of the wing increased, tends to discount this possibility. Furthermore, the tuft photographs in figure 18 show that the fences did not eliminate spanwise flow of the boundary-layer air, although there is some indication that they reduced it.

The stabilizing effect of the fences appears to be most logically explained on the premise that they increased the lift developed by the outer sections of the wing (those sections to the rear of the moment center). From a practical point of view, it would seem that at least a portion of the boundary-layer air approaching a fence from the inboard side was deflected off the wing, although this effect is not evident from the tuft photographs in figure 18. The tuft photographs do show, however, that the most pronounced boundary-layer-flow changes resulting from the addition of the fences occurred in a localized area just outboard of each fence, the tuft behavior in these regions appearing to be very similar to that near the wing root. It is surmised that these sections behaved in a manner similar to those near the root of the wing developing higher than normal lift coefficients as a result of the boundary-layer control afforded by the spanwise flow outboard of the fence.

CONCLUDING REMARKS

The results of wind-tunnel tests of a semispan model of a high aspect ratio swept-back wing and a fuselage have been presented. On the basis of the findings of past research, the wing was designed to have sections incorporating camber, twist, and generous leading-edge radii in an effort to attain satisfactory longitudinal stability characteristics by the elimination of premature separation of the flow near the leading edge at moderate and high lift coefficients. The tuft photographs presented herein demonstrate that the initial point of flow separation was well back from the leading edge. With this type of flow, it was found that fences, properly located on the upper surface of the wing, markedly improved the longitudinal stability and the high-lift

characteristics of the wing. It is believed that the effectiveness of these fences was at least partly attributable to the absence of leading-edge-type separation as a result of the use of camber, twist, and adequate leading-edge radii.

At a Mach number of 0.165 and Reynolds number of 8,000,000, the use of fences limited the variation of pitching-moment-curve slope to less than 0.10 for lift coefficients up to 1.33. Without fences, a large decrease of longitudinal stability began at a lift coefficient of about 0.9. At all higher test Mach numbers, the longitudinal stability of the wing-fuselage combination with fences on the wing was nearly constant up to a lift coefficient of at least 0.60. The addition of the fences increased the lift-drag ratios at the higher lift coefficients but had little or no effect on the minimum drag or the Mach number for drag divergence. Of significance with regard to the range capabilities of a high-speed airplane of the type considered is the fact that a lift-drag ratio of 23 was attained for the wing-fuselage combination at a Mach number of 0.83 and a lift coefficient of 0.45.

It was found that estimates of a number of the important aerodynamic parameters by use of available theoretical methods were in good agreement with the experimental values.

Ames Aeronautical Laboratory
National Advisory Committee for Aeronautics
Moffett Field, Calif.

REFERENCES

1. Hunton, Lynn W.: Effects of Twist and Camber on the Low-Speed Characteristics of a Large-Scale 45° Swept-back Wing. NACA RM A50A10, 1950.
2. Johnson, Ben H., Jr., and Shibata, Harry H.: Characteristics Throughout the Subsonic Speed Range of a Plane Wing and of a Cambered and Twisted Wing, Both Having 45° of Sweepback. NACA RM A51D27, 1951.
3. Tinling, Bruce E., and Kolk, W. Richard: The Effects of Mach Number and Reynolds Number on the Aerodynamic Characteristics of Several 12-Percent-Thick Wings Having 35° of Sweepback and Various Amounts of Camber. NACA RM A50K27, 1951.
4. Kelly, John A.: Effects of Modifications to the Leading-Edge Region on the Stalling Characteristics of the NACA 63₁-012 Airfoil Section. NACA TN 2228, 1950.

5. Demele, Fred A., and Sutton, Fred B.: The Effects of Increasing the Leading-Edge Radius and Adding Forward Camber on the Aerodynamic Characteristics of a Wing With 35° of Sweepback. NACA RM A50K28a, 1951.
6. Edwards, George G., and Boltz, Frederick W.: An Analysis of the Forces and Pressure Distribution on a Wing With the Leading-Edge Swept Back 37.25° . NACA RM A9K01, 1950.
7. Summers, James L., and Treon, Stuart L.: The Effects of Amount and Type of Camber on the Variation With Mach Number of the Aerodynamic Characteristics of a 10-Percent-Thick NACA 64A-Series Airfoil Section. NACA TN 2096, 1950.
8. Nitzberg, Gerald E., Crandall, Stewart M., and Polentz, Perry P.: A Preliminary Investigation of the Usefulness of Camber in Obtaining Favorable Airfoil-Section Drag Characteristics at Supercritical Speeds. NACA RM A9G20, 1949.
9. Loftin, Laurence K., Jr.: Theoretical and Experimental Data for a Number of NACA 6A-Series Airfoil Sections. NACA Rep. 903, 1948. (Formerly NACA TN 1368)
10. DeYoung, John, and Harper, Charles W.: Theoretical Symmetric Span Loading at Subsonic Speeds for Wings Having Arbitrary Plan Form. NACA Rep. 921, 1948. (Formerly NACA TN's 1476, 1491, and 1772)
11. Abbott, Ira H., von Doenhoff, Albert E., and Stivers, Louis S., Jr.: Summary of Airfoil Data. NACA Rep. 824, 1945.
12. Herriot, John G.: Blockage Corrections for Three-Dimensional-Flow Closed-Throat Wind Tunnels with Consideration of the Effect of Compressibility. NACA Rep. 995, 1950. (Formerly NACA RM A7B28)
13. Sivells, James C., and Salmi, Rachel M.: Jet-Boundary Corrections for Complete and Semispan Swept Wings in Closed Circular Wind Tunnels. NACA TN 2454, 1951.
14. Hunton, Lynn W., and Dew, Joseph K.: The Effects of Camber and Twist on the Aerodynamic Loading and Stalling Characteristics of a Large-Scale 45° Swept-Back Wing. NACA RM A50J24, 1951.

TABLE I.- FUSELAGE COORDINATES

Distance from nose (in.)	Radius (in.)
0	0
1.27	1.04
2.54	1.57
5.08	2.35
10.16	3.36
20.31	4.44
30.47	4.90
39.44	5.00
50.00	5.00
60.00	5.00
70.00	5.00
76.00	4.96
82.00	4.83
88.00	4.61
94.00	4.27
100.00	3.77
106.00	3.03
126.00	0

NACA

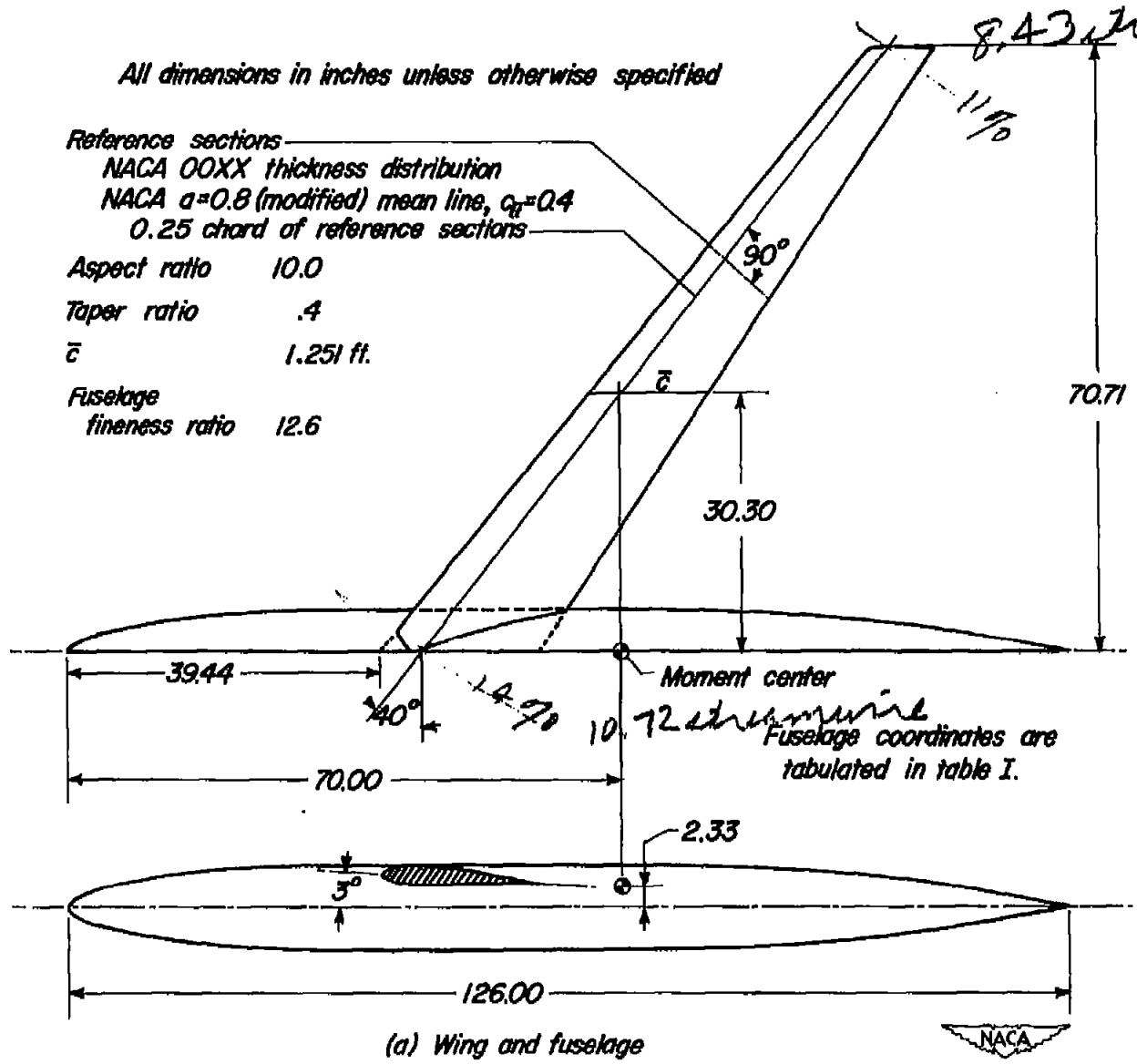
~~CONFIDENTIAL~~

NACA RM A52F18

All dimensions in inches unless otherwise specified

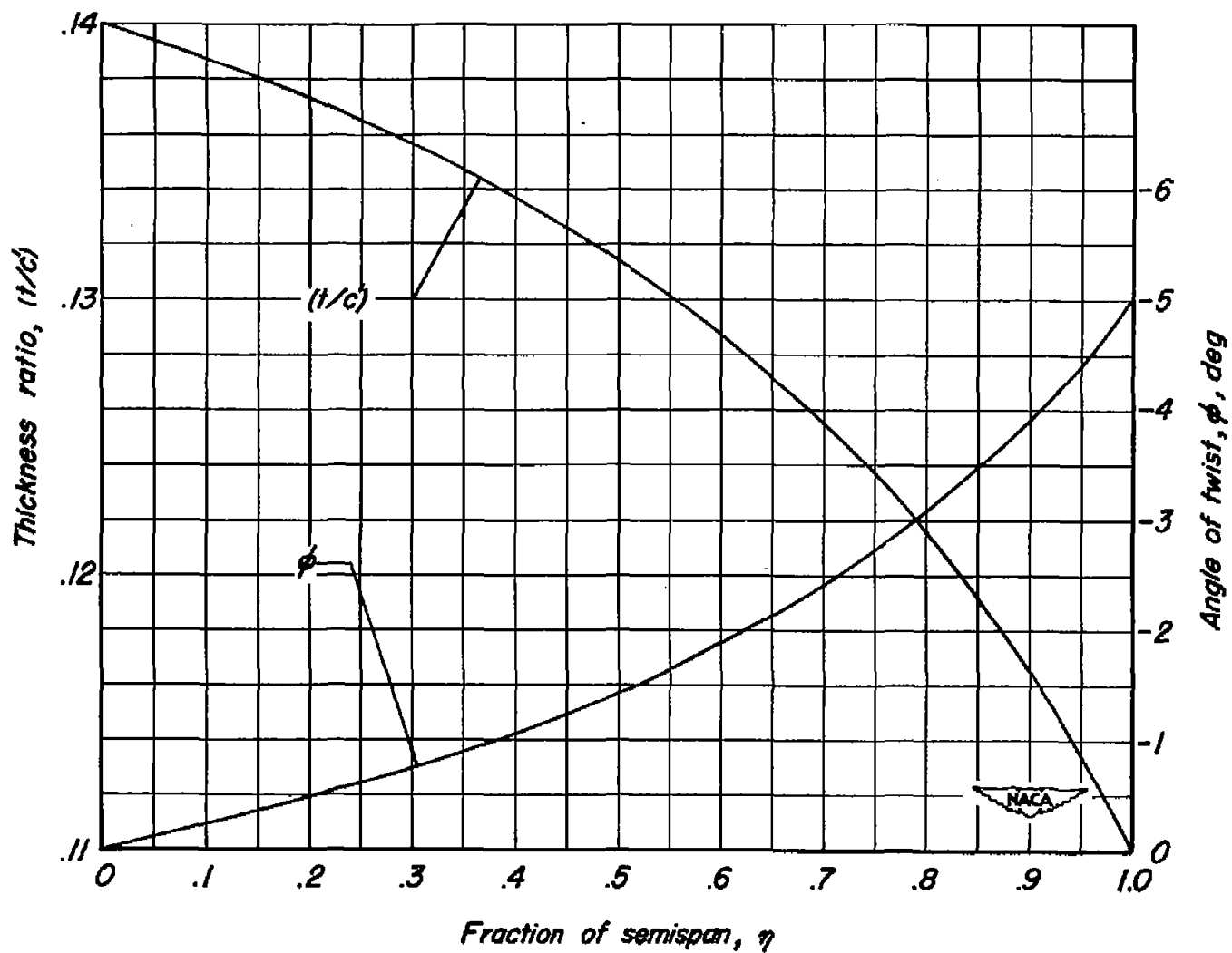
Reference sections
NACA 00XX thickness distribution
NACA a=0.8 (modified) mean line, $c_{tr}=0.4$
0.25 chord of reference sections

Aspect ratio 10.0
Taper ratio .4
 \bar{c} 1.251 ft.
Fuselage fineness ratio 12.6



(a) Wing and fuselage

Figure 1.- Geometry of the model.



(b) Distribution of twist and thickness ratio.

Figure 1. - Concluded.

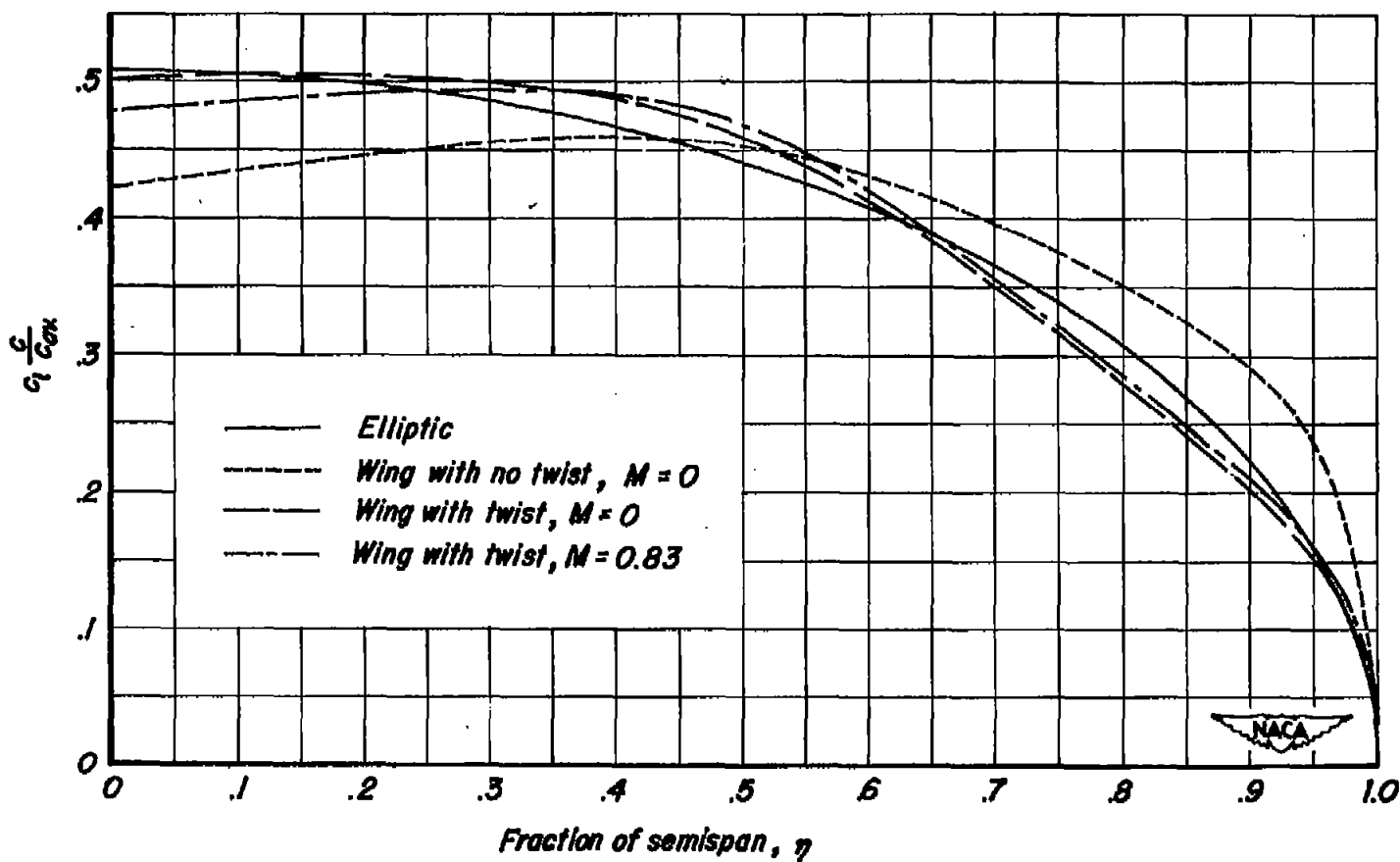
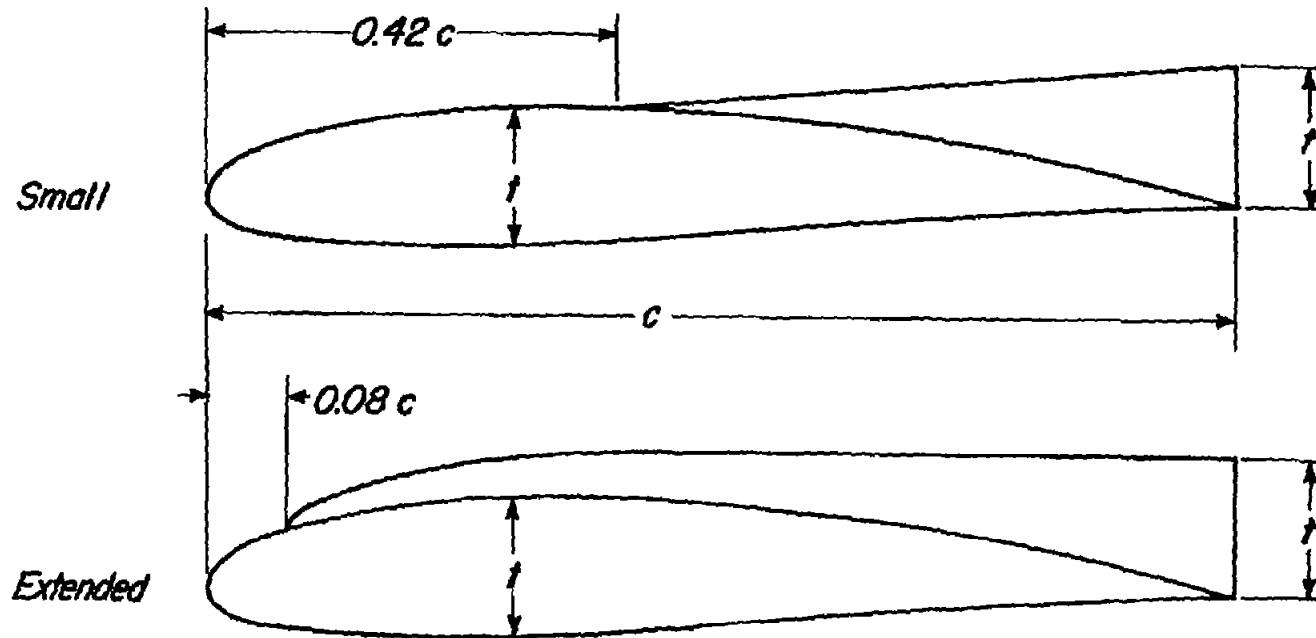


Figure 2.- The theoretical spanwise distribution of $\frac{c_l}{c_{l_{av}}}$ calculated by the Weissinger method for a lift coefficient of 0.4.



Type	Small			Extended		
Fence	A	B	C	D	E	F
Spanwise location, η	0.33	0.50	0.75	0.50	0.70	0.85

Figure 3.— Fence details.



(a) Wing-fuselage model in the wind tunnel.



(b) Details of the fences.

Figure 4.- Photographs of the model.

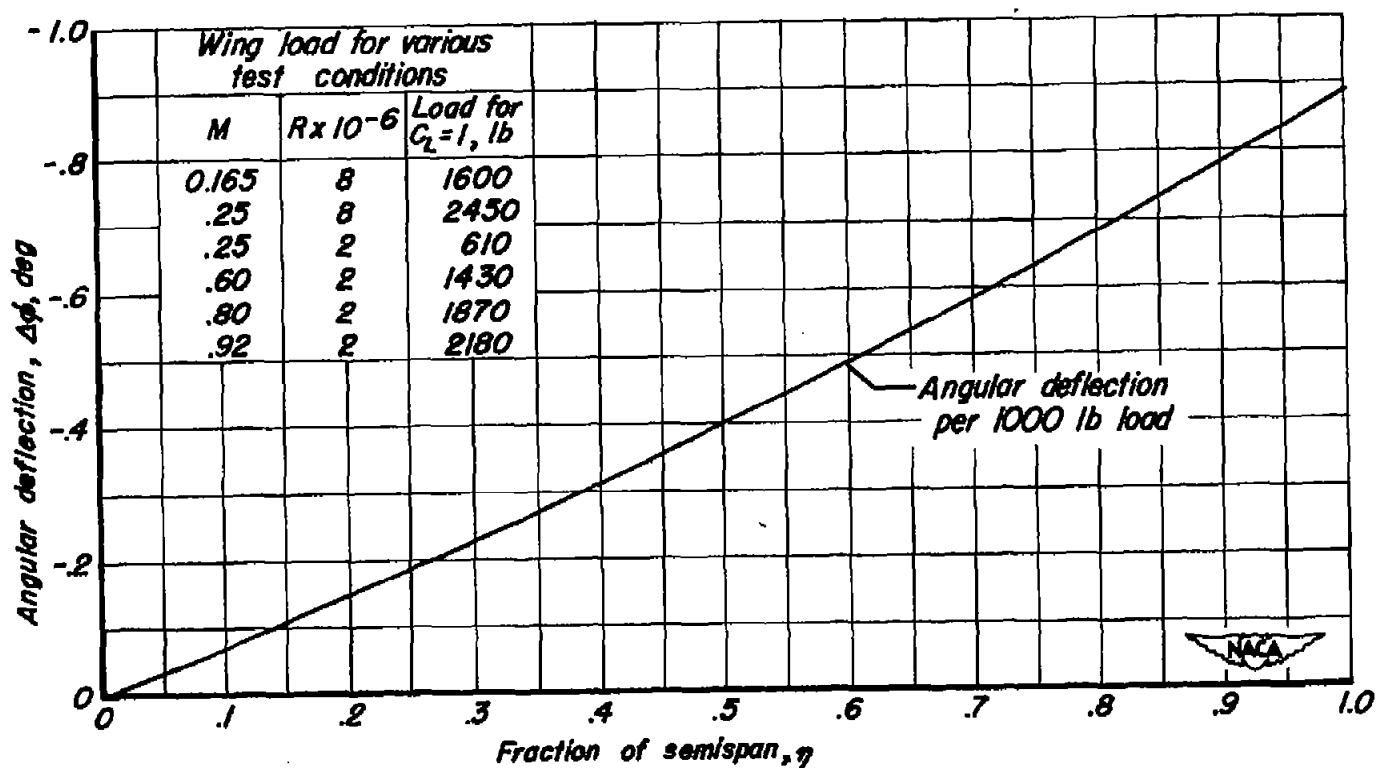


Figure 5.— Angular deflection due to wing bending based on the theoretical span-loading for $C_L=1.0$.

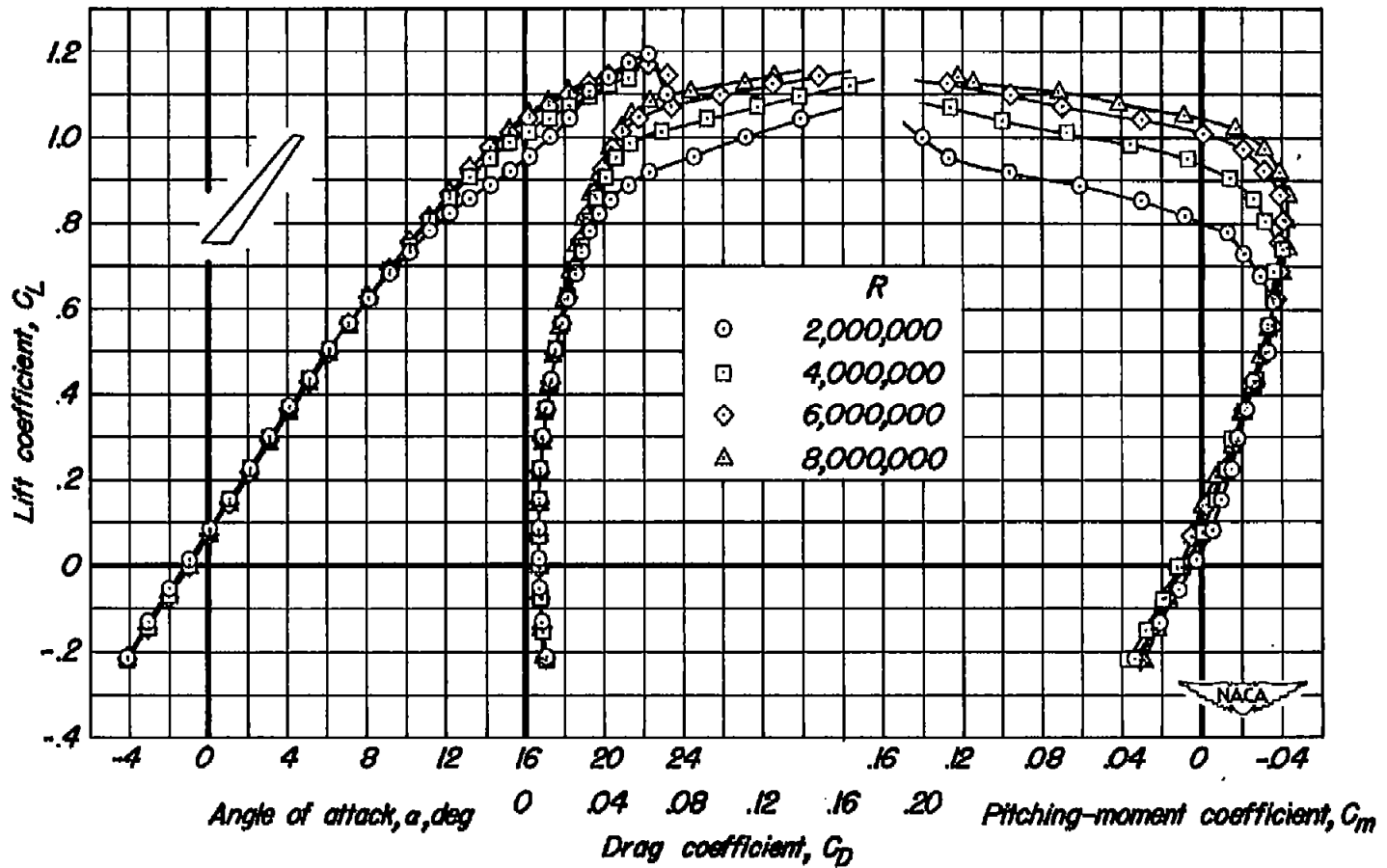


Figure 6.— The effect of Reynolds number on the lift, drag, and pitching-moment coefficients of the wing alone. $M=0.25$.

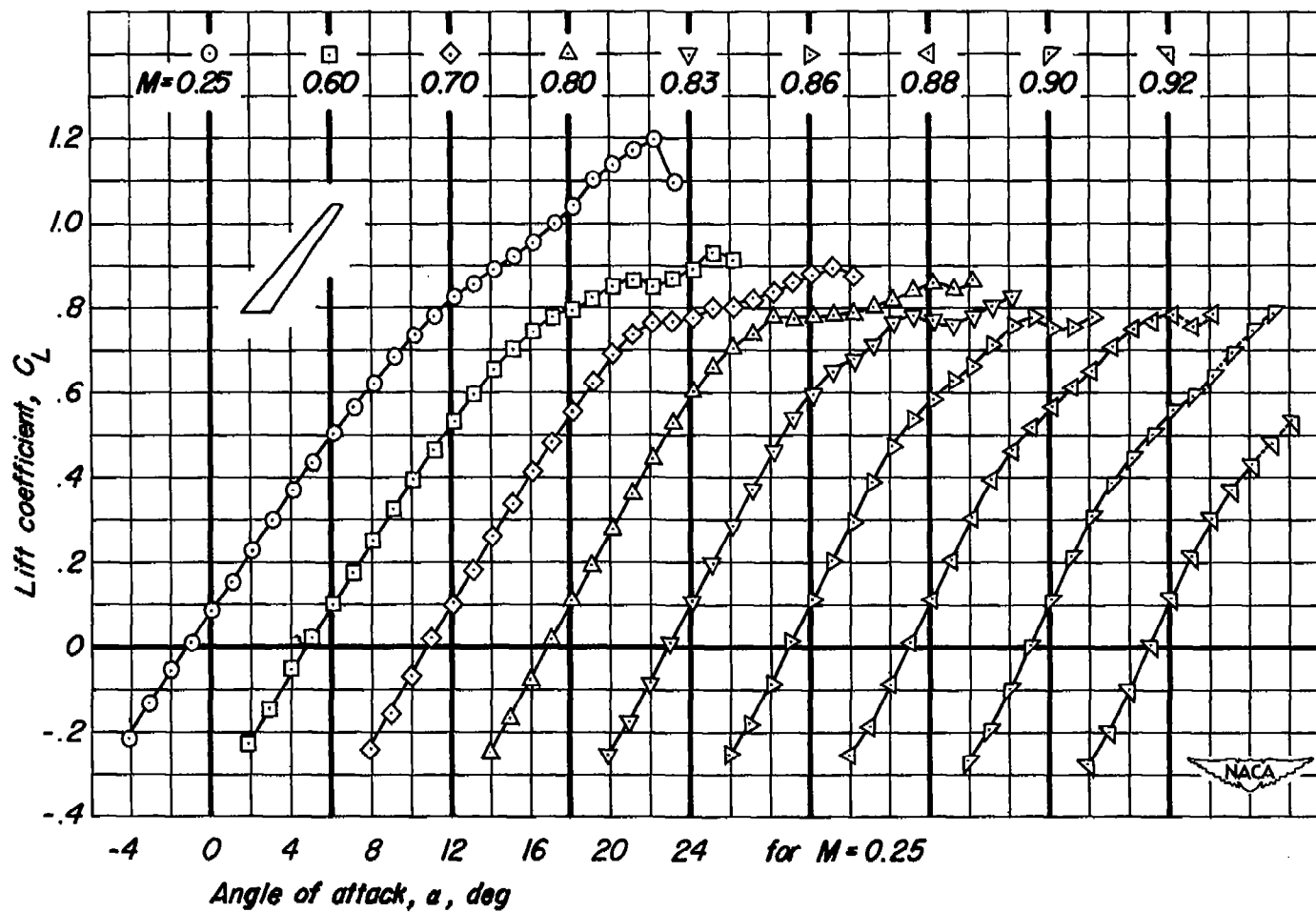
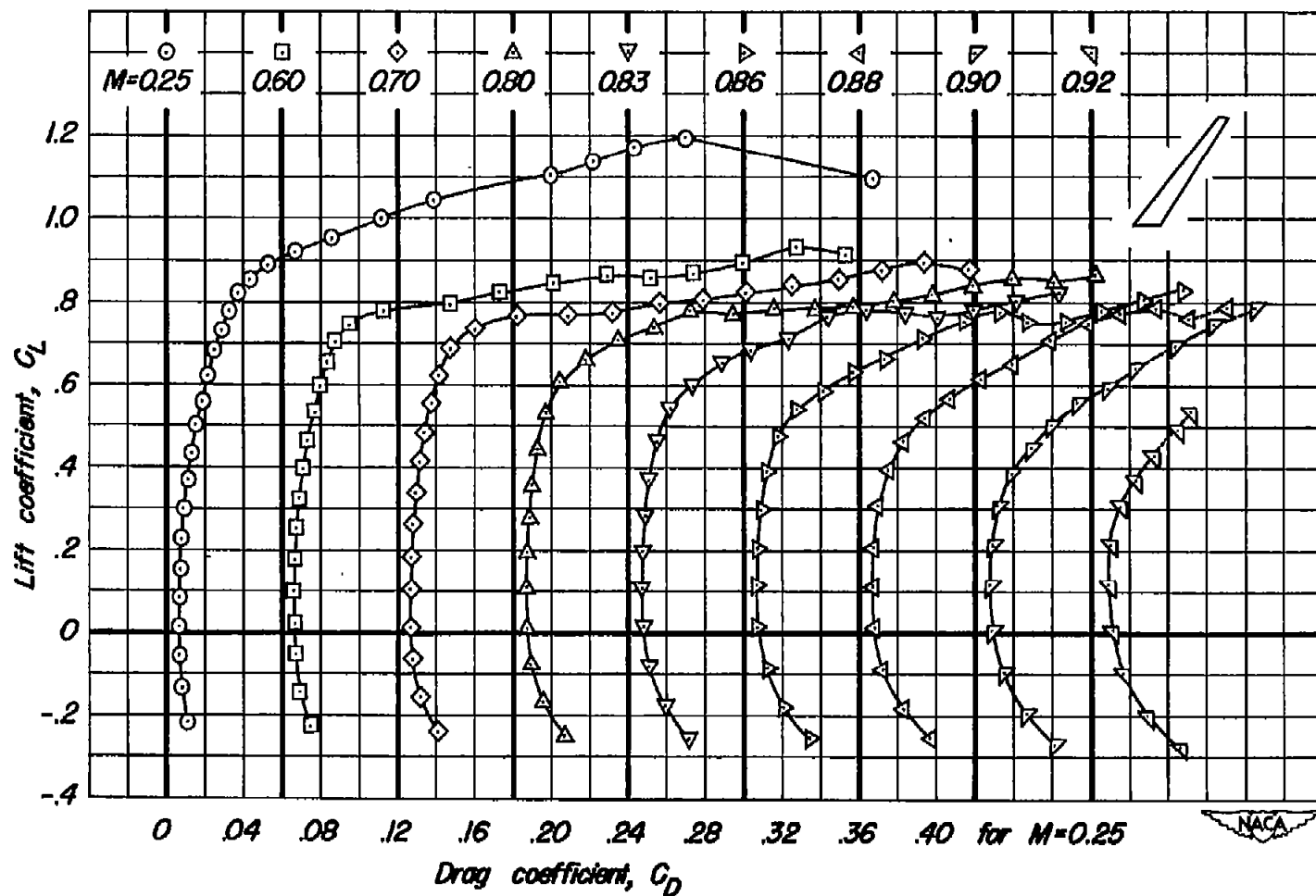
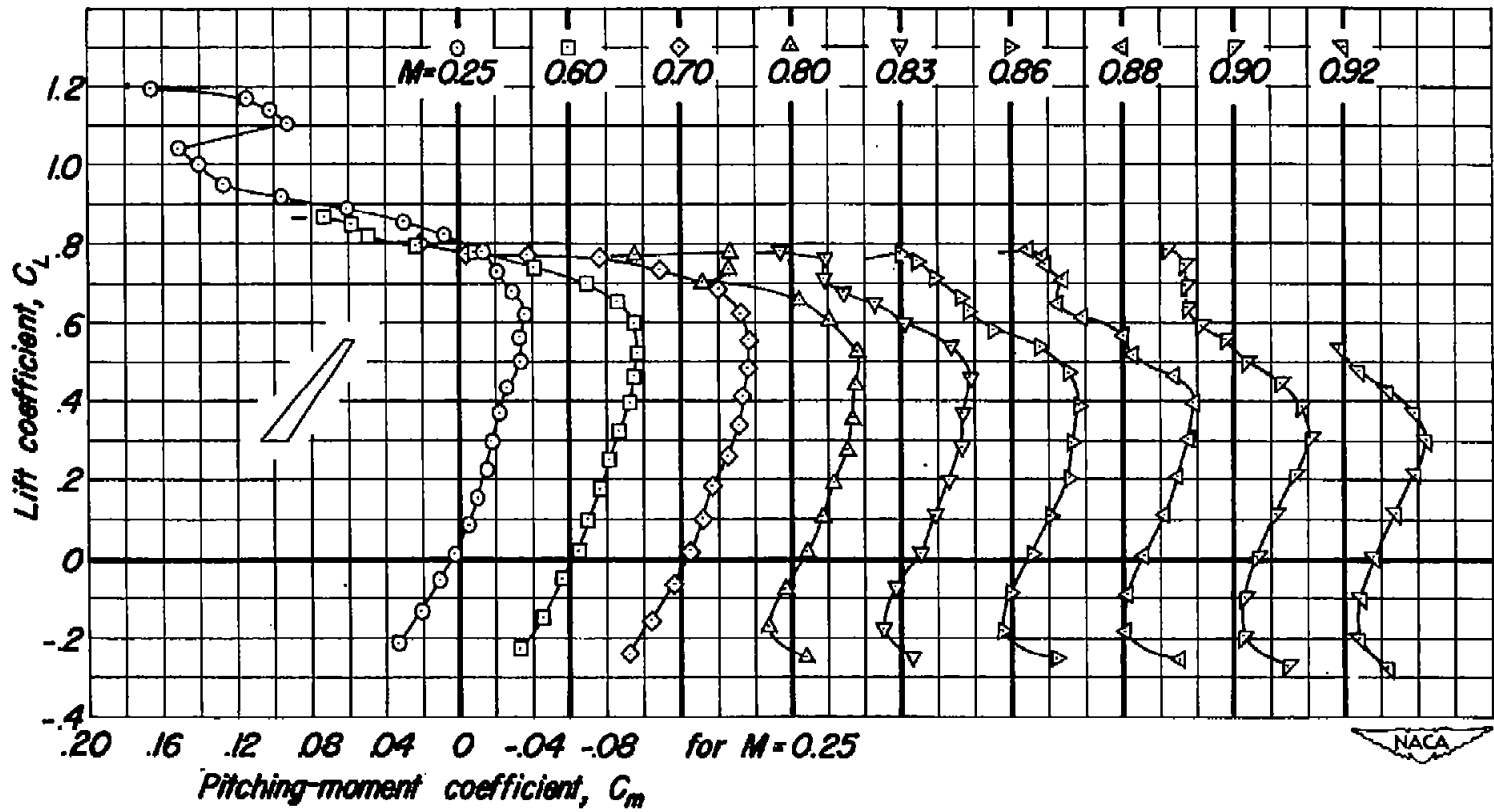
(a) C_L vs α

Figure 7.—The effect of Mach number on the lift, drag, and pitching-moment coefficients of the wing alone. $R=2,000,000$.



(b) C_L vs C_D

Figure 7.- Continued.



(c) C_L vs C_m

Figure 7.- Concluded.

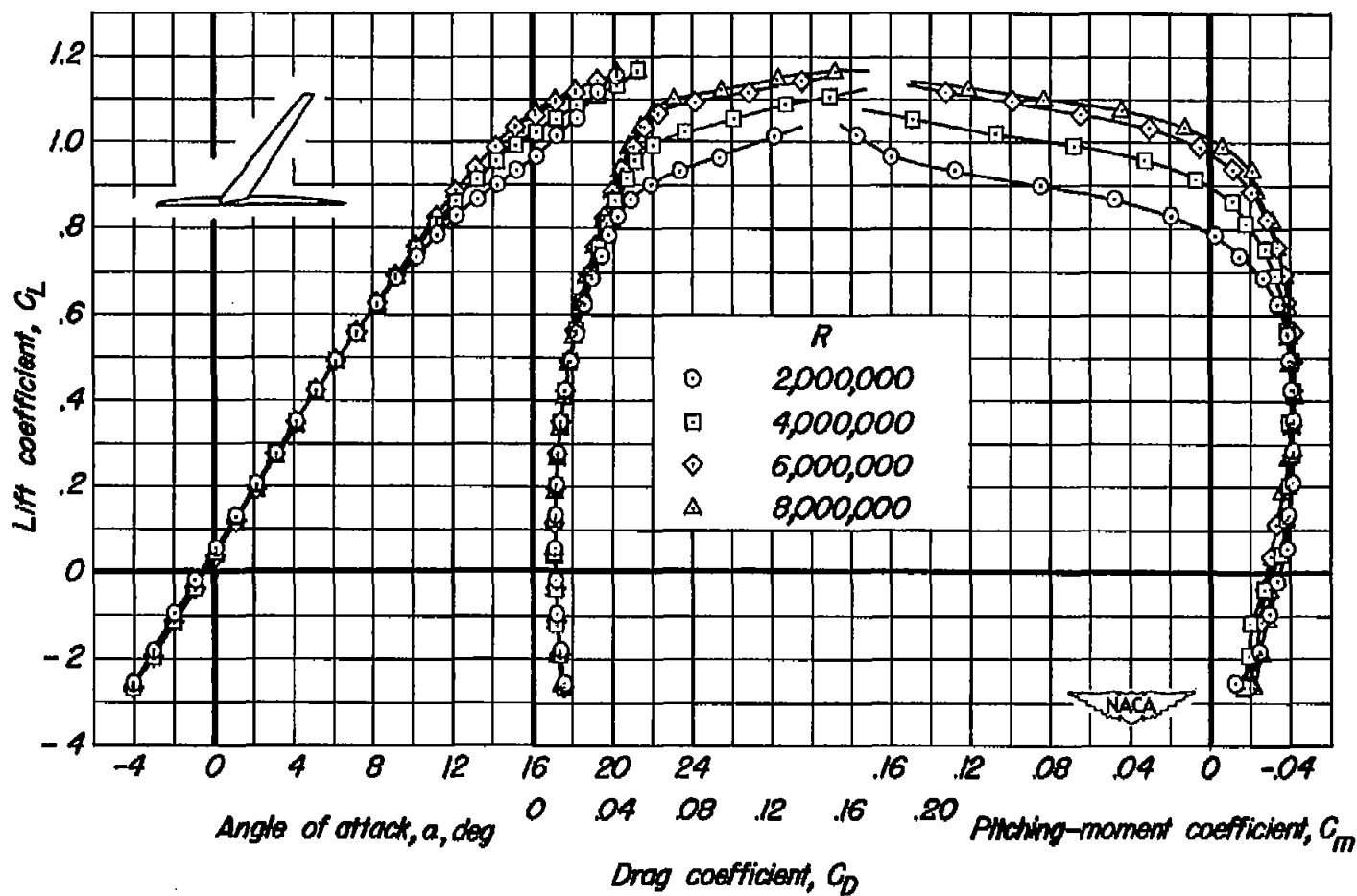
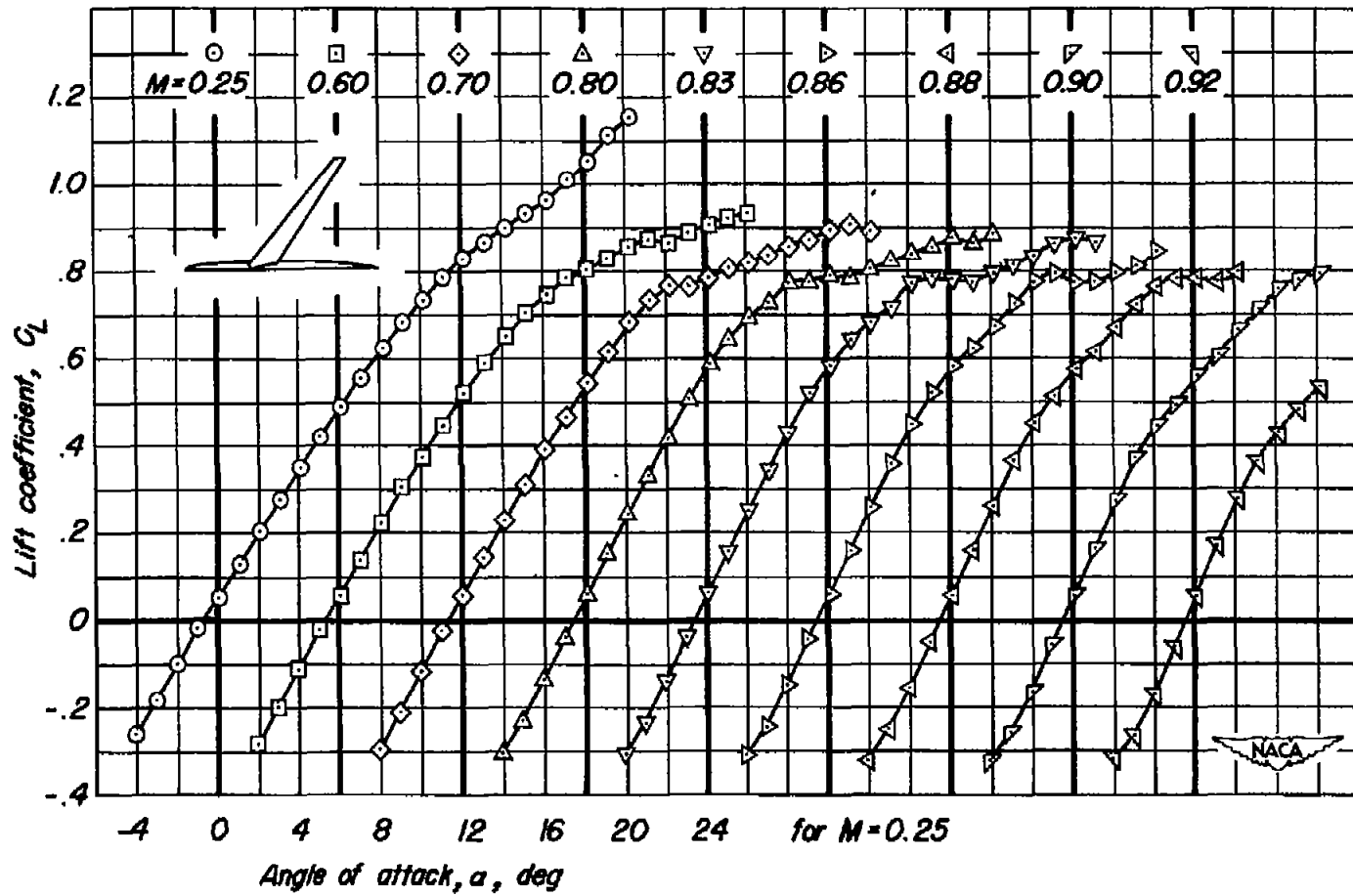
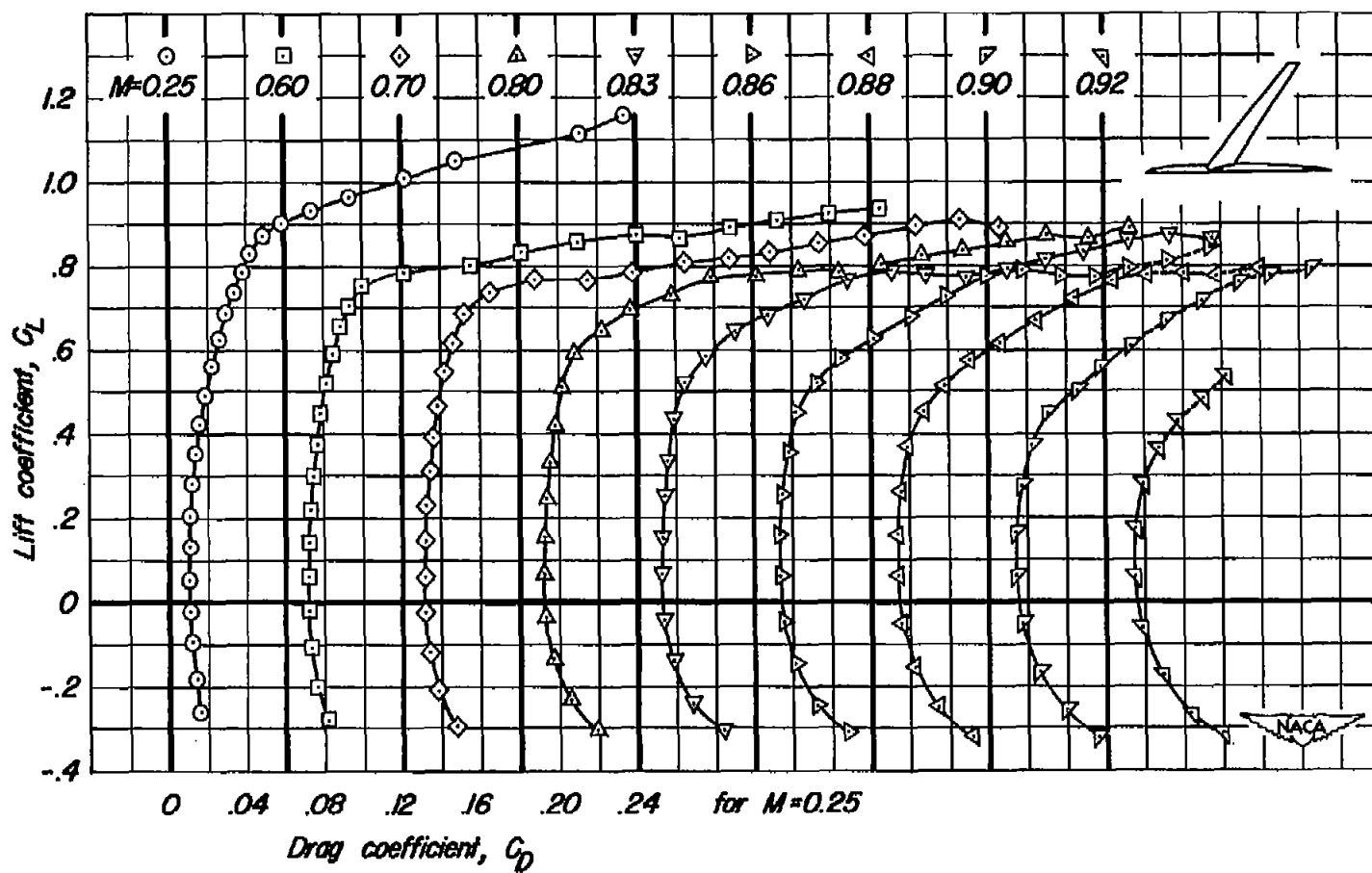


Figure 8.— The effect of Reynolds number on the lift, drag, and pitching-moment coefficients of the wing-fuselage combination. $M=0.25$.

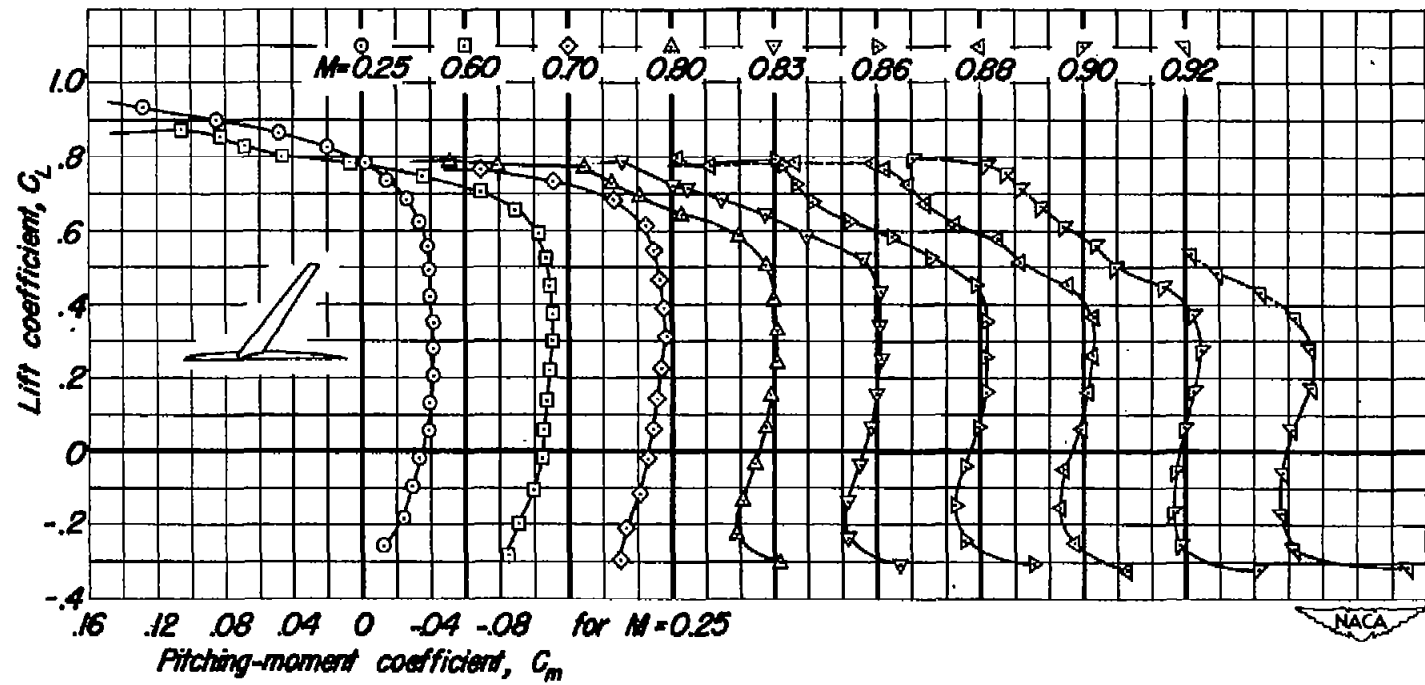


(a) C_L vs a

Figure 9.— The effect of Mach number on the lift, drag, and pitching-moment coefficients of the wing-fuselage combination. $R=2,000,000$.



(b) C_L vs C_D
 Figure 9.—Continued.



(c) C_L vs C_m
Figure 9.— Concluded.

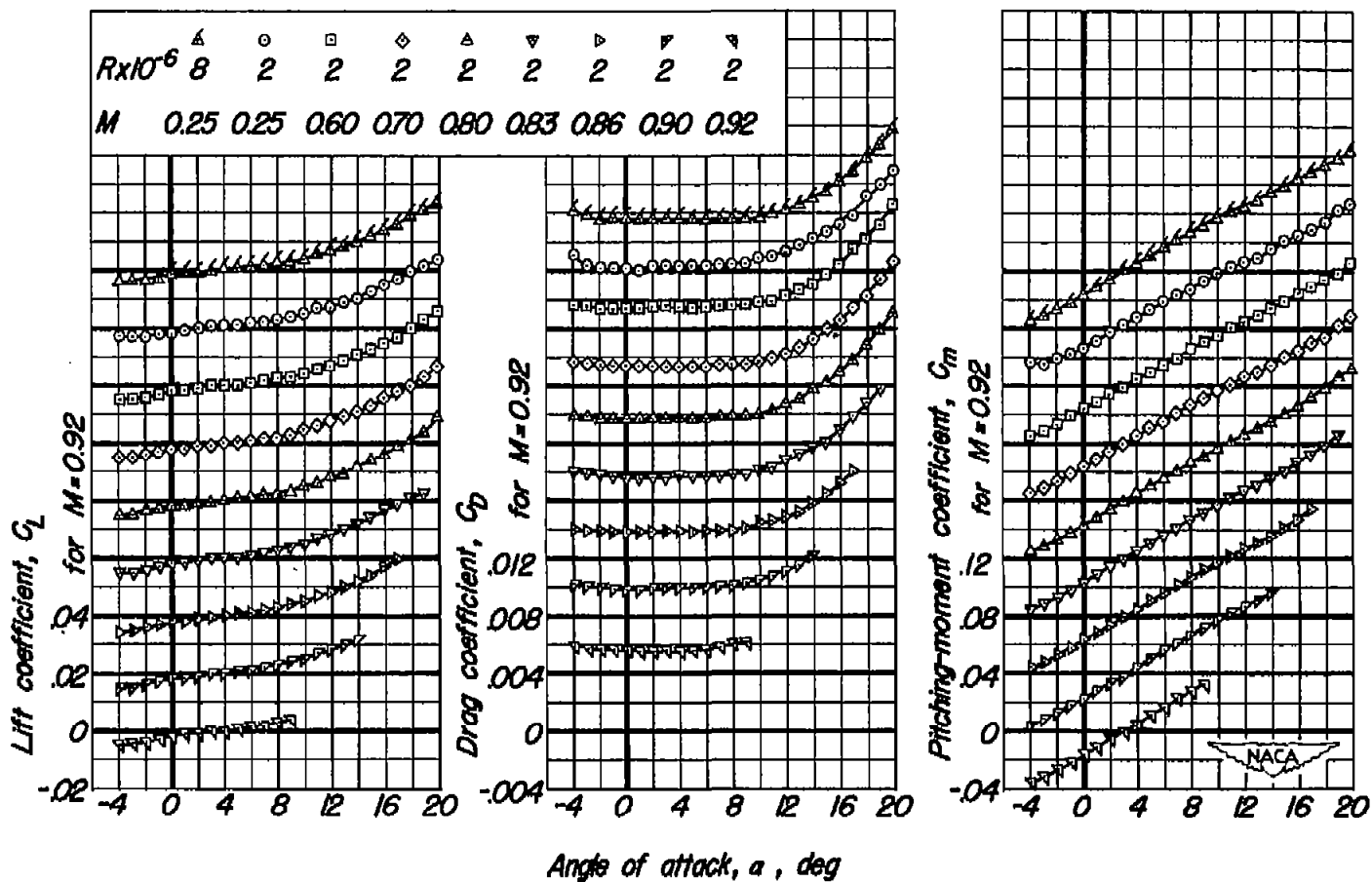
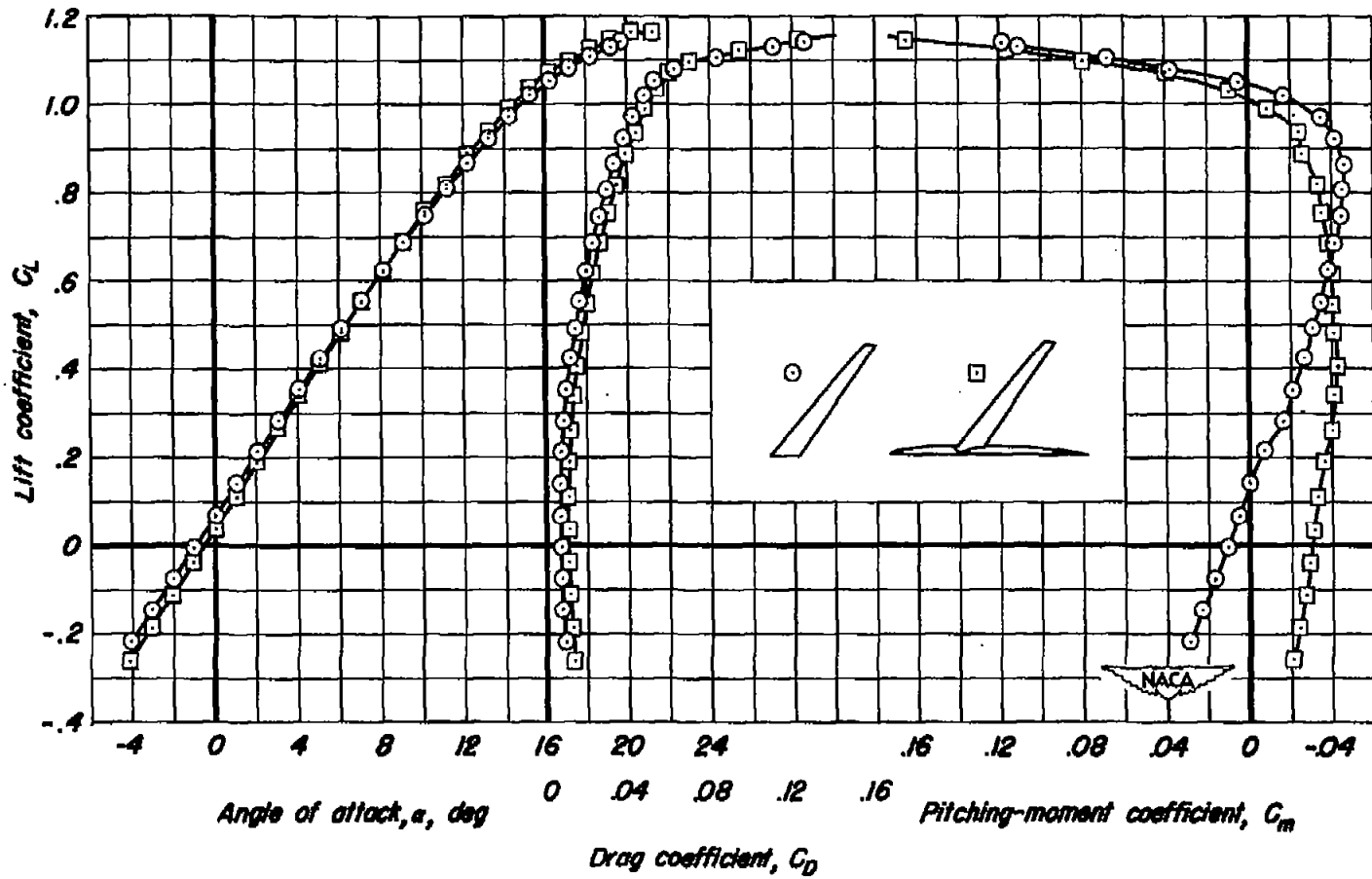
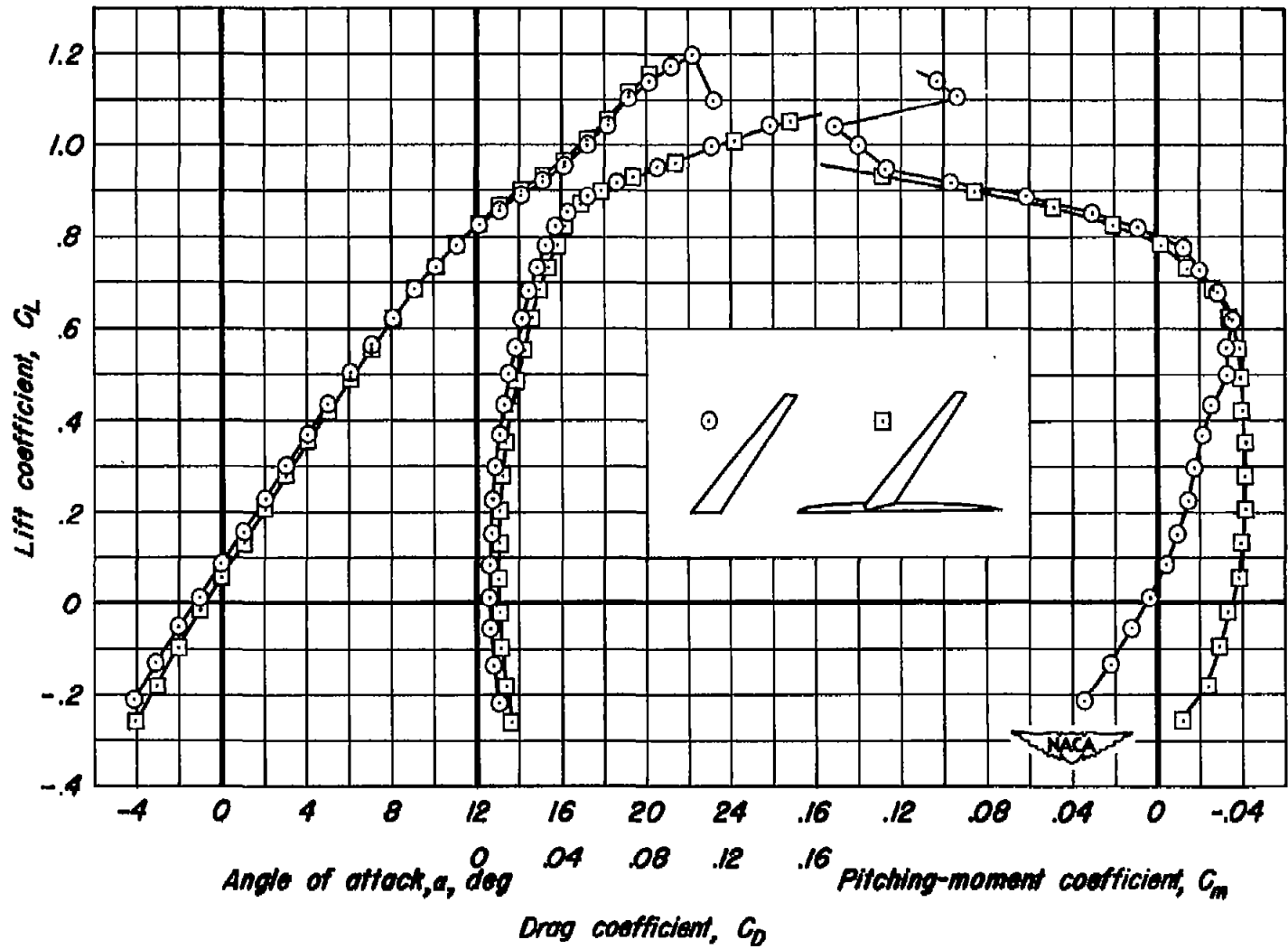


Figure 10.- The lift, drag, and pitching-moment coefficients of the fuselage.

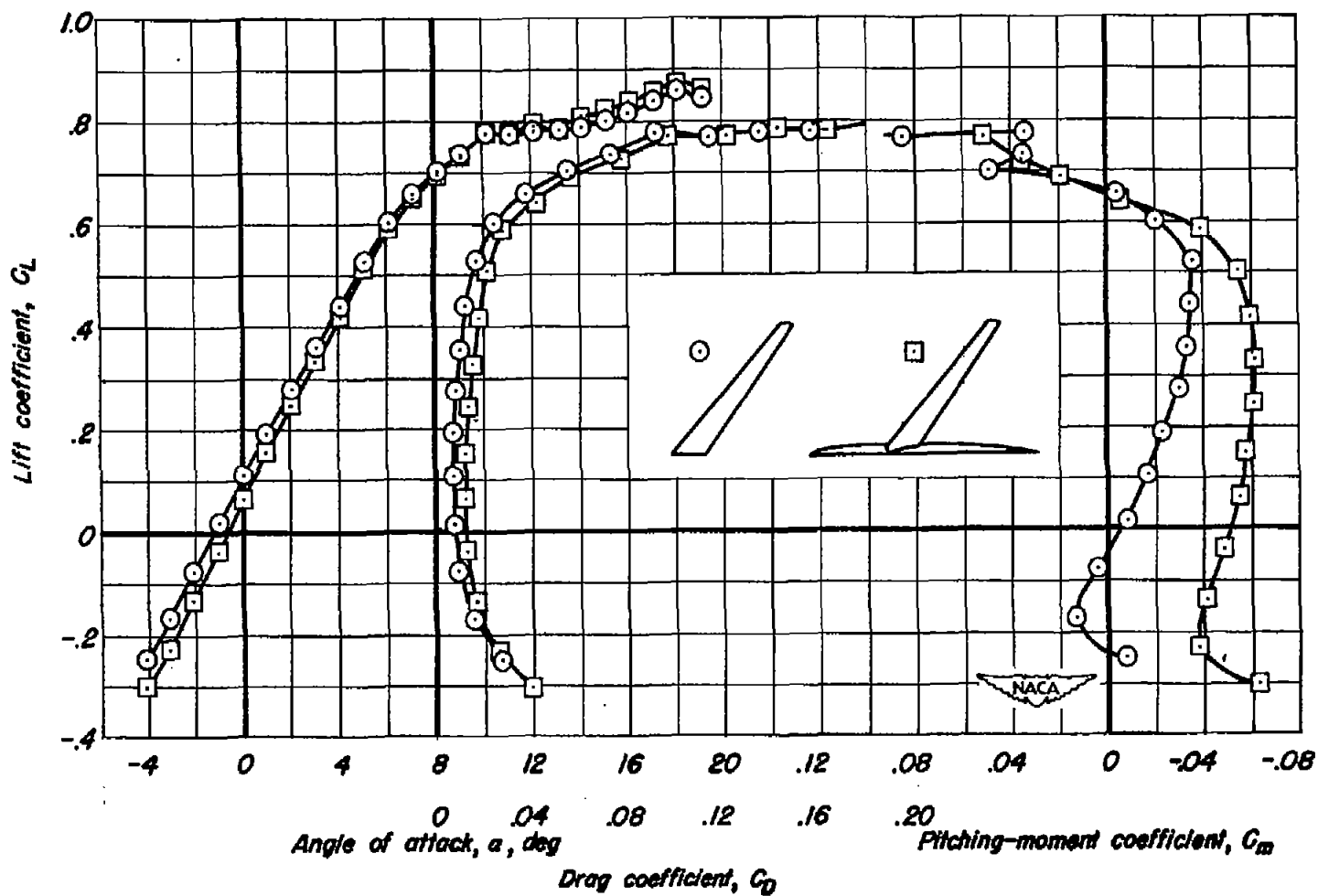


(a) $M=0.25$, $R=8,000,000$

Figure 11.- The lift, drag, and pitching-moment coefficients of the wing alone and of the wing-fuselage combination.

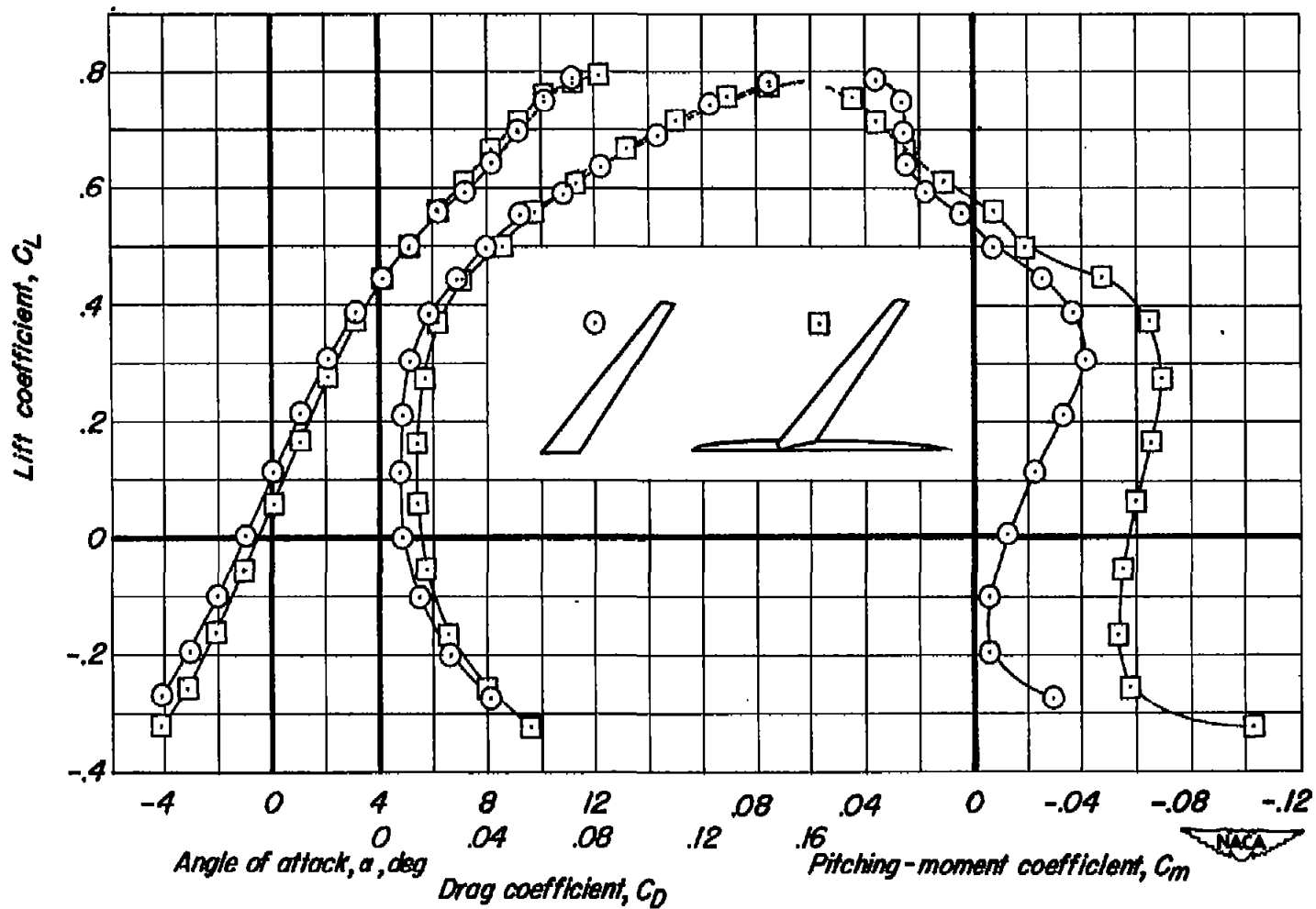


(b) $M = 0.25, R = 2,000,000$
 Figure 11.— Continued.



(c) $M=0.80$, $R=2,000,000$.

Figure 11.-Continued.



(d) $M=0.90$, $R=2,000,000$
 Figure 11.— Concluded.

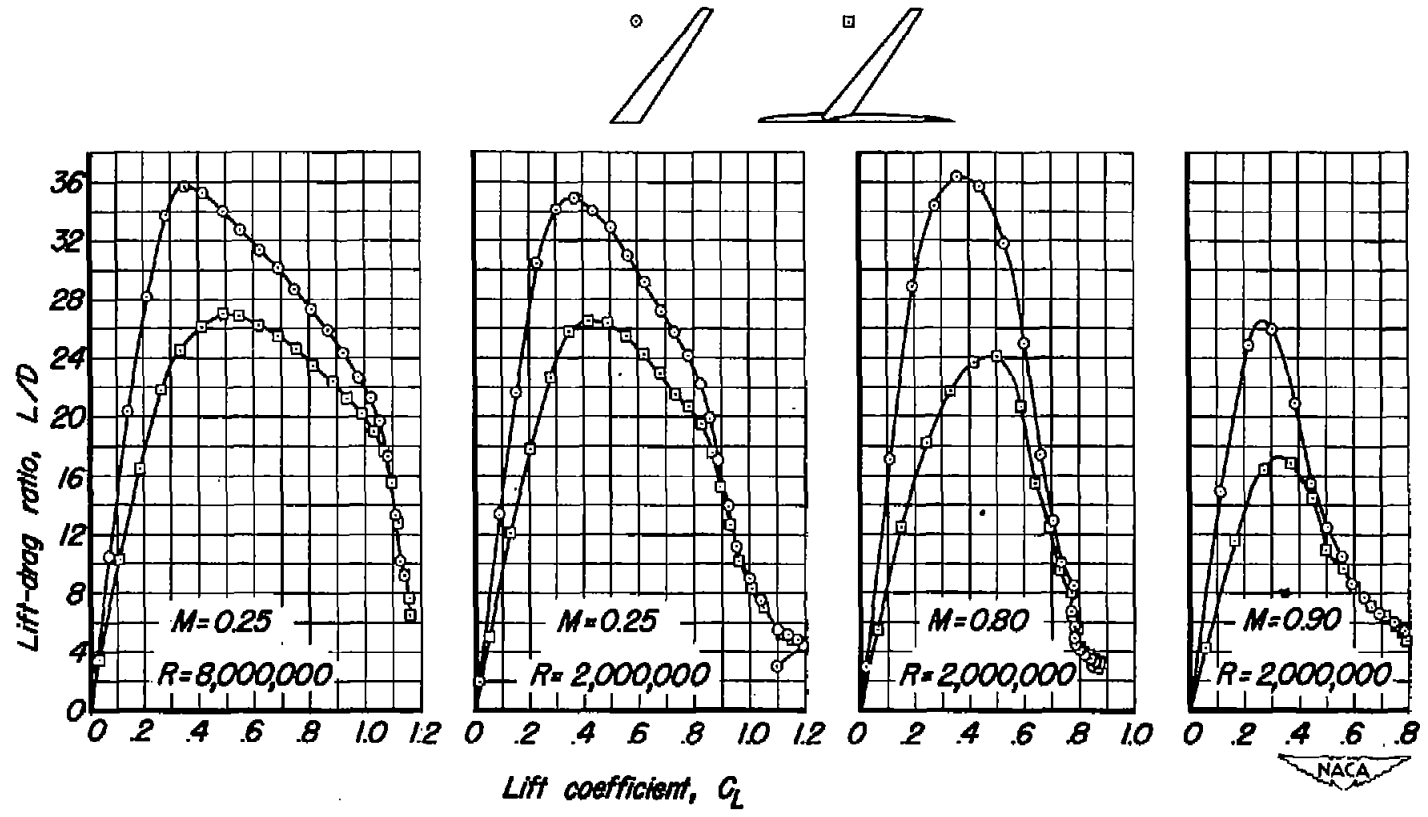


Figure 12.— The effect of the fuselage on the lift-drag ratio.

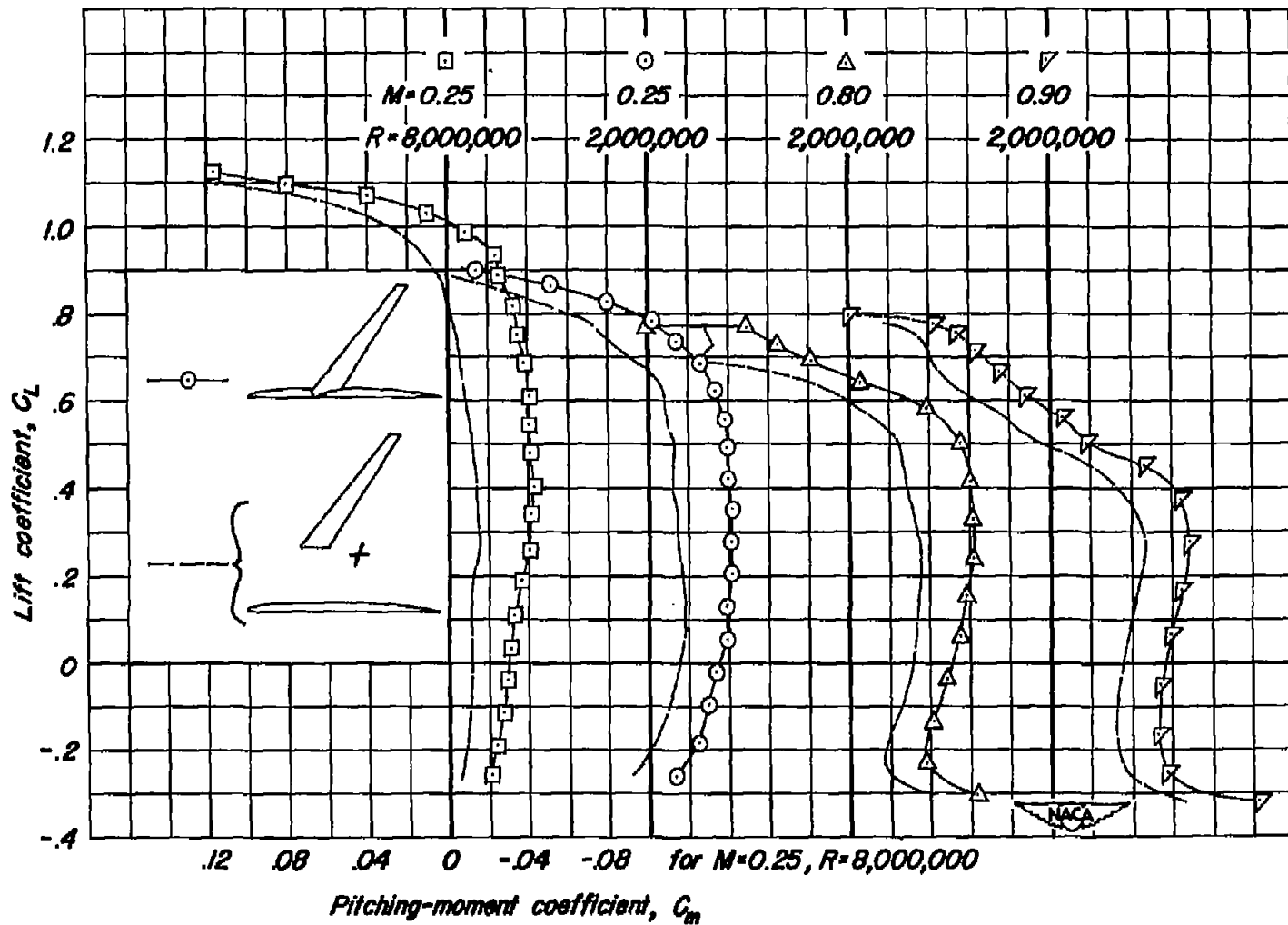


Figure 13.— Comparison of the pitching-moment coefficients of the wing-fuselage combination with the sum of the pitching-moment coefficients of the wing alone and the fuselage.

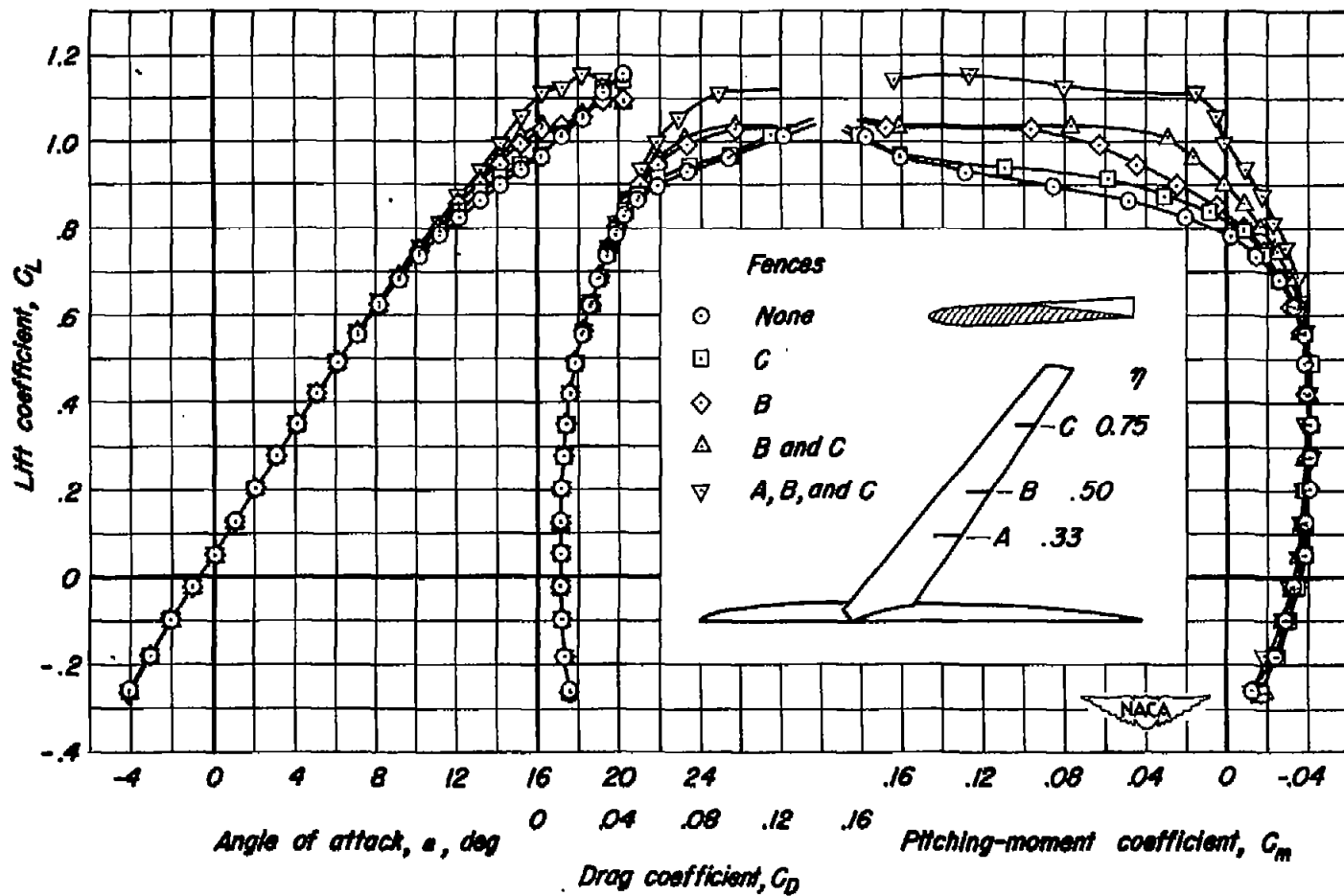
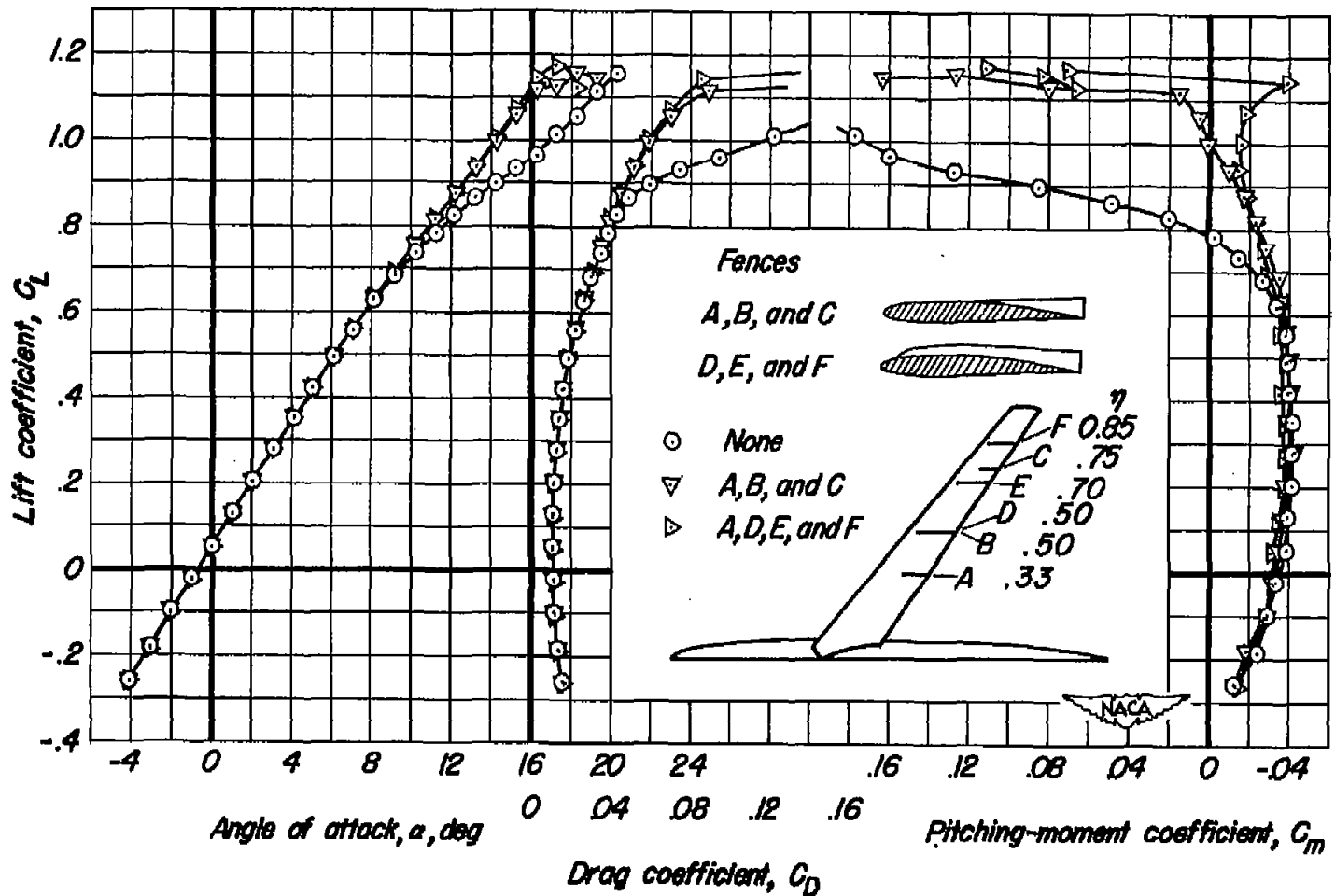
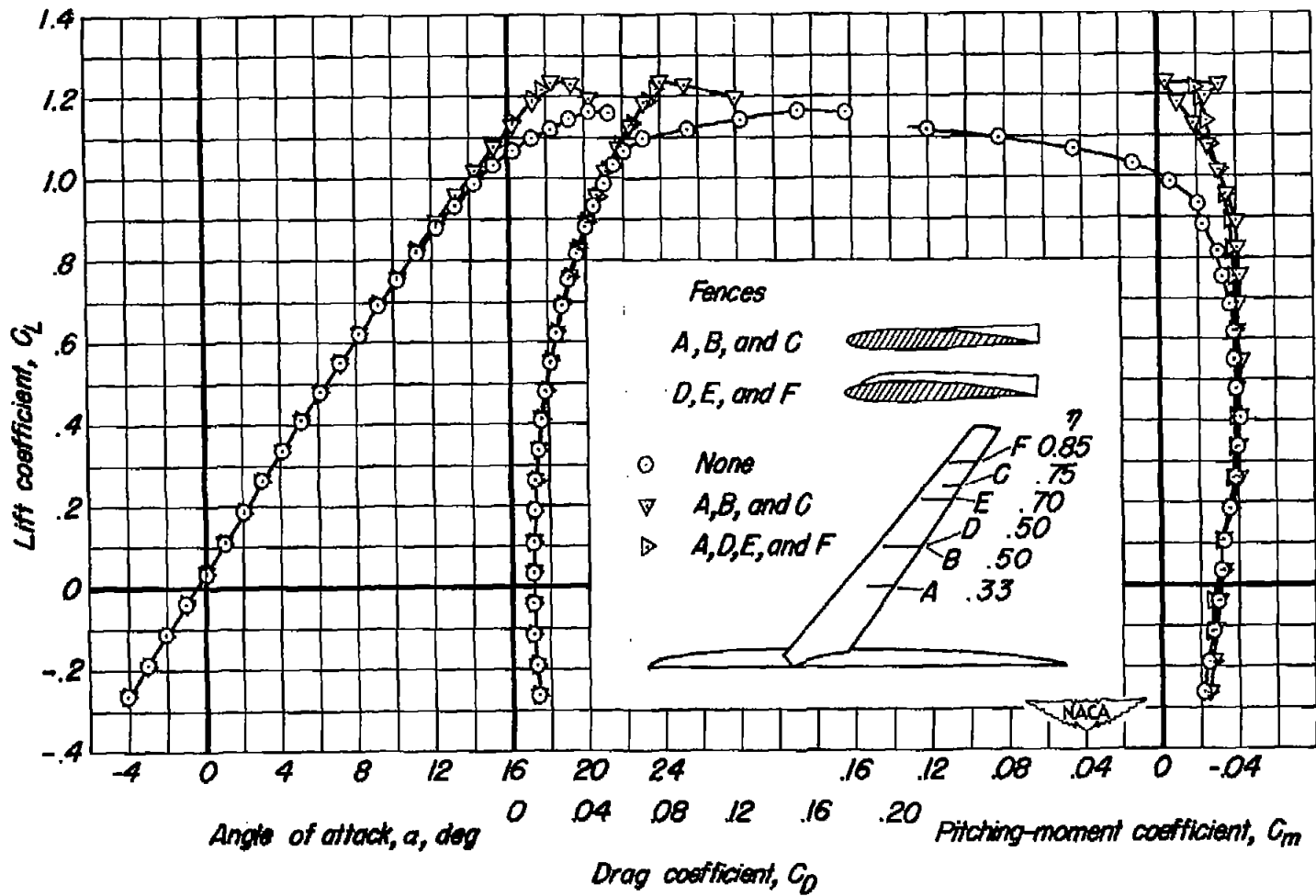


Figure 14.— The effect of several arrangements of small fences on the lift, drag, and pitching-moment coefficients of the wing-fuselage combination. $M=0.25$, $R=2,000,000$.



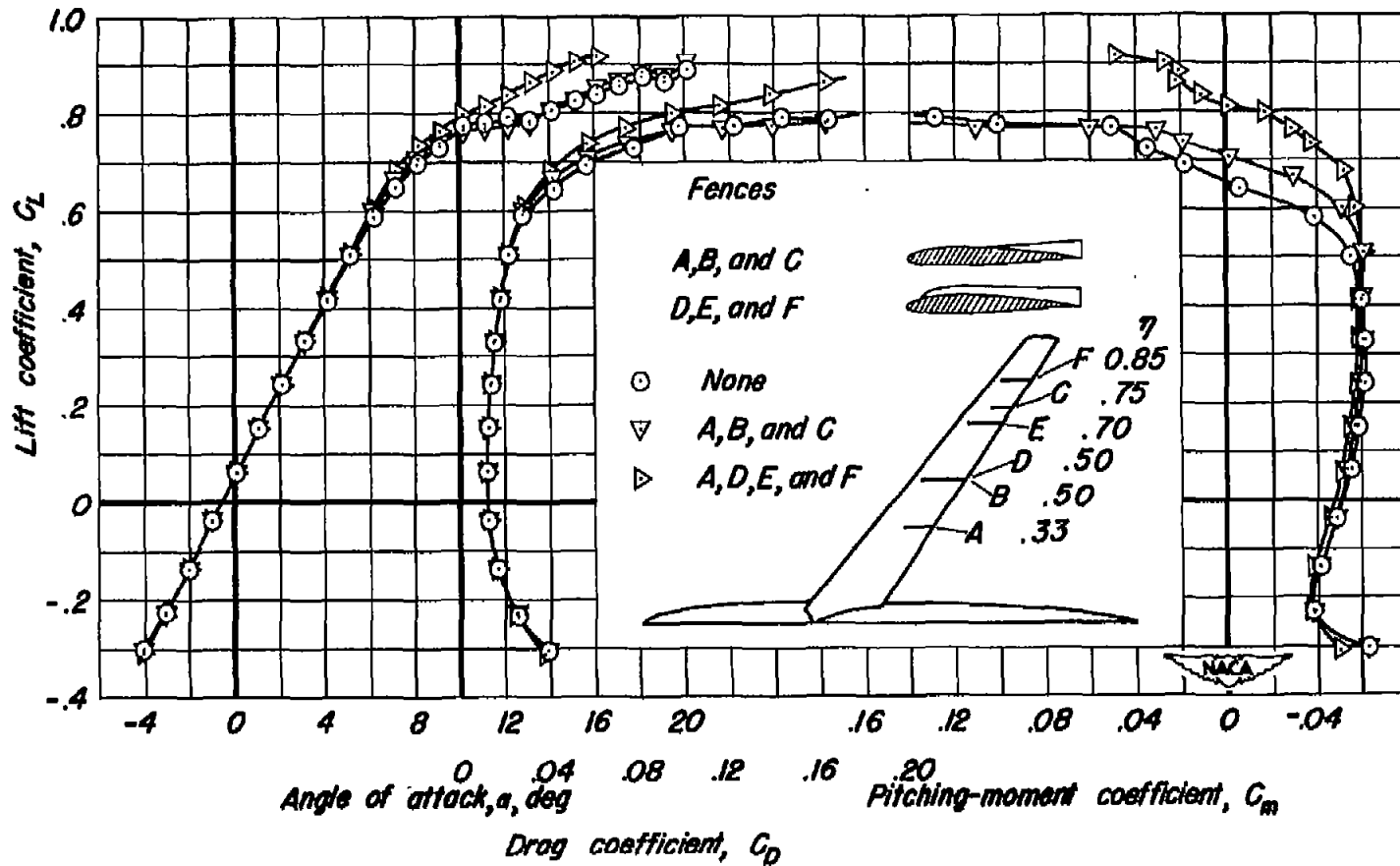
(a) $M=0.25, R=2,000,000$

Figure 15.— The effect of two fence configurations on the lift, drag, and pitching-moment coefficients of the wing-fuselage combination.



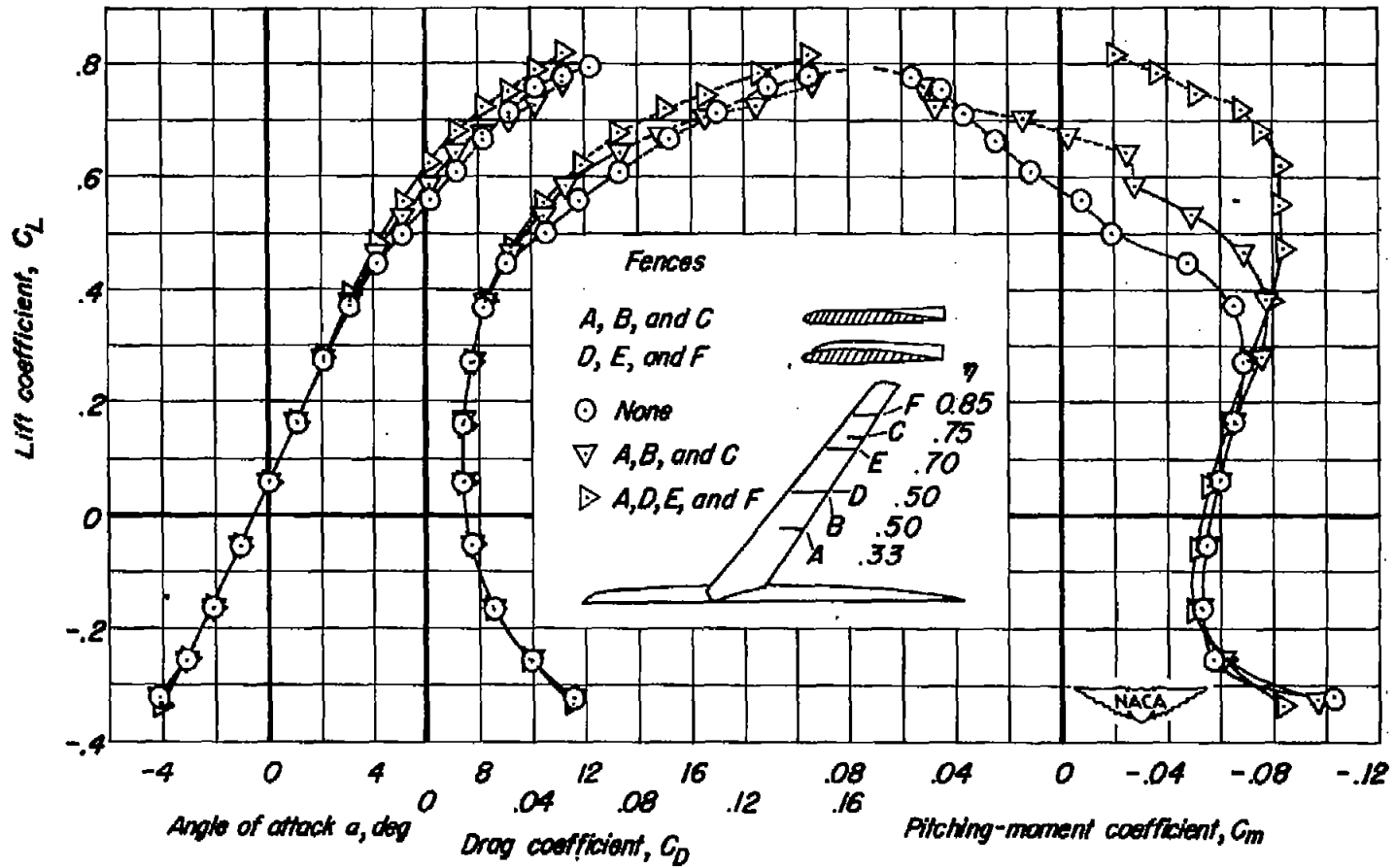
(b) $M=0.25, R=8,000,000$

Figure 15.—Continued.



(c) $M = 0.80, R = 2,000,000$

Figure 15-- Continued.



(d) $M=0.90$, $R=2,000,000$
Figure 15.—Concluded.

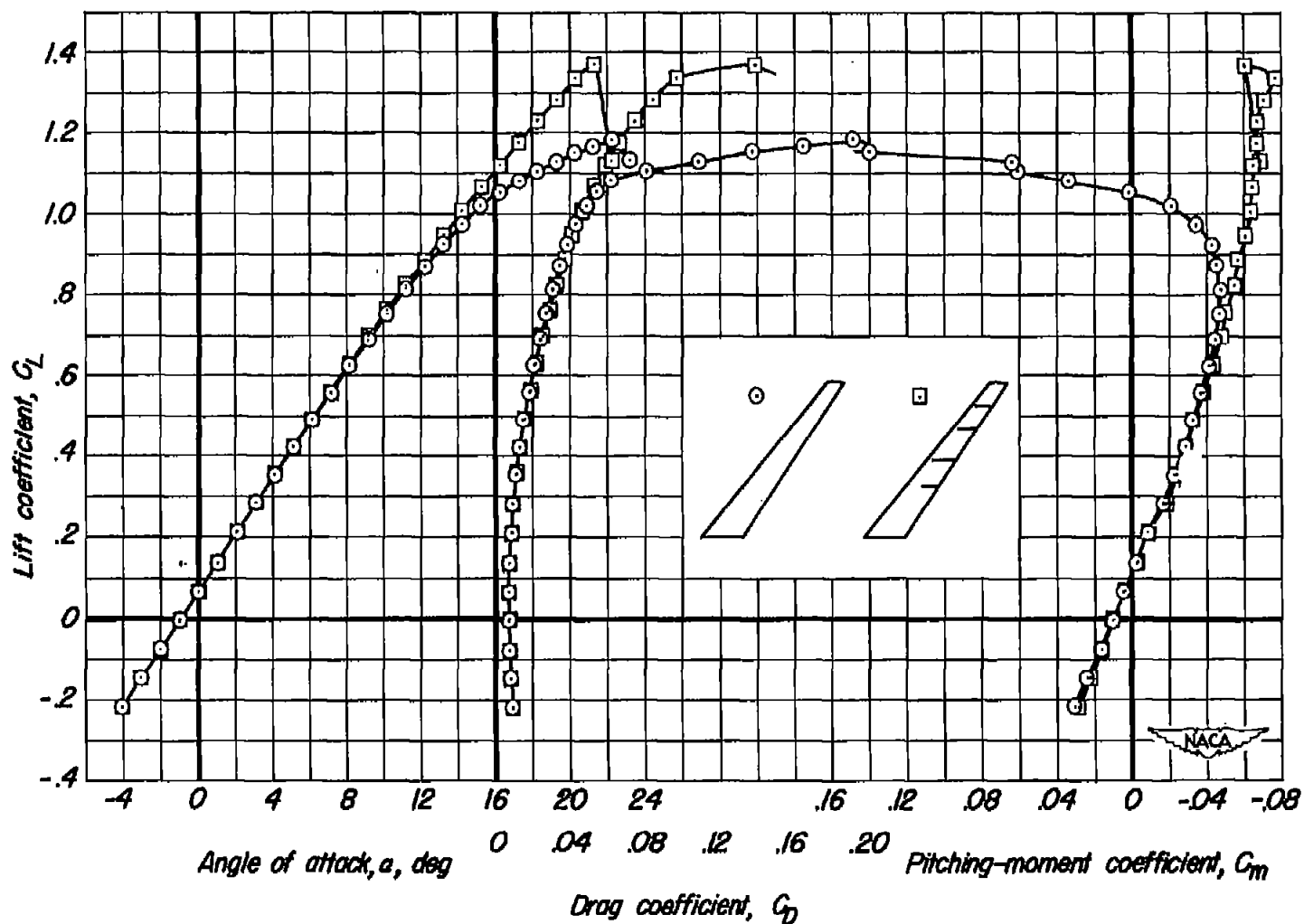


Figure 16.—The effect of four fences (one small fence at $\eta = 0.33$ and extended fences at $\eta = 0.50, 0.70$ and 0.85) on the lift, drag, and pitching-moment coefficients of the wing alone. $M = 0.165, R = 8,000,000$.

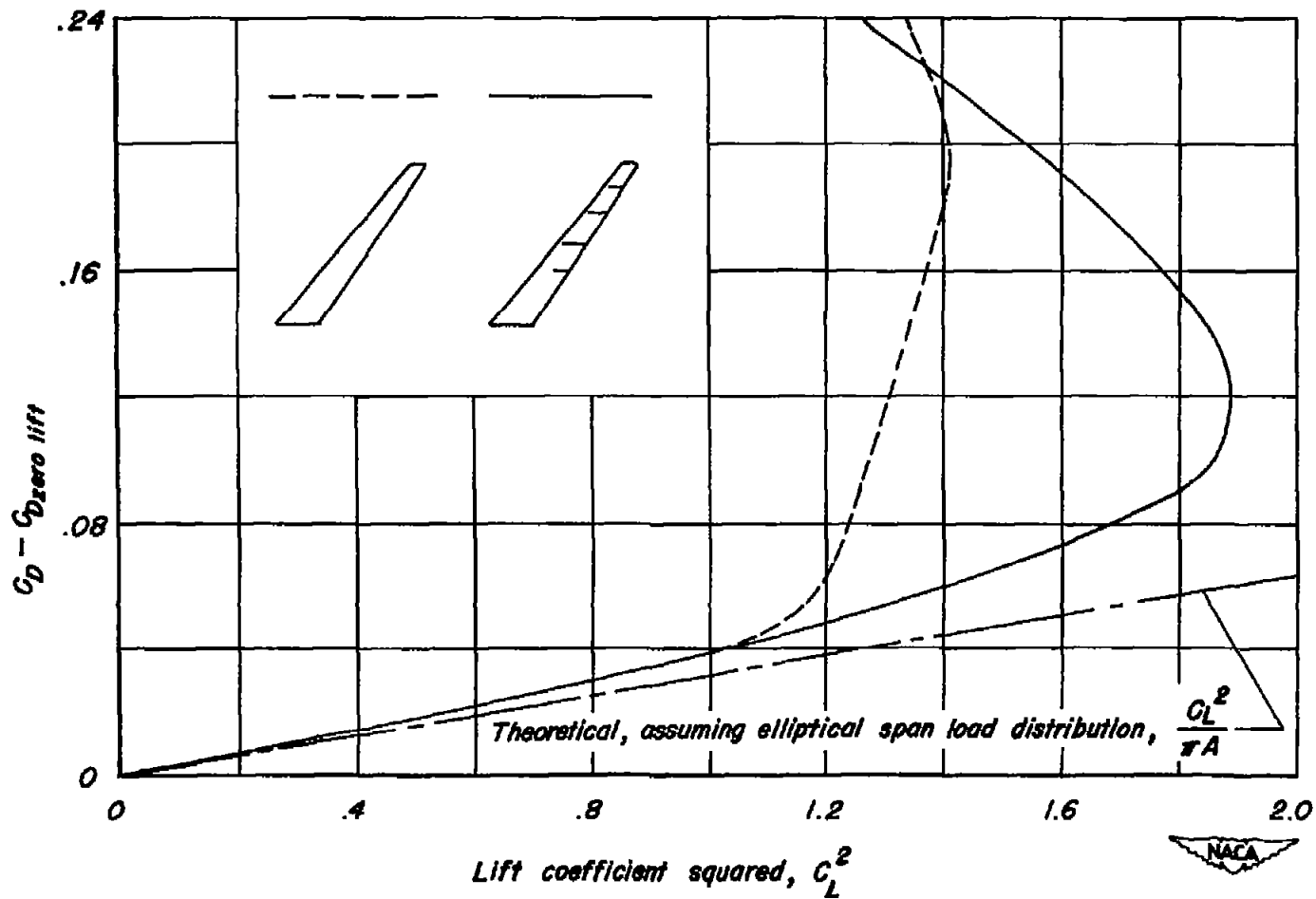
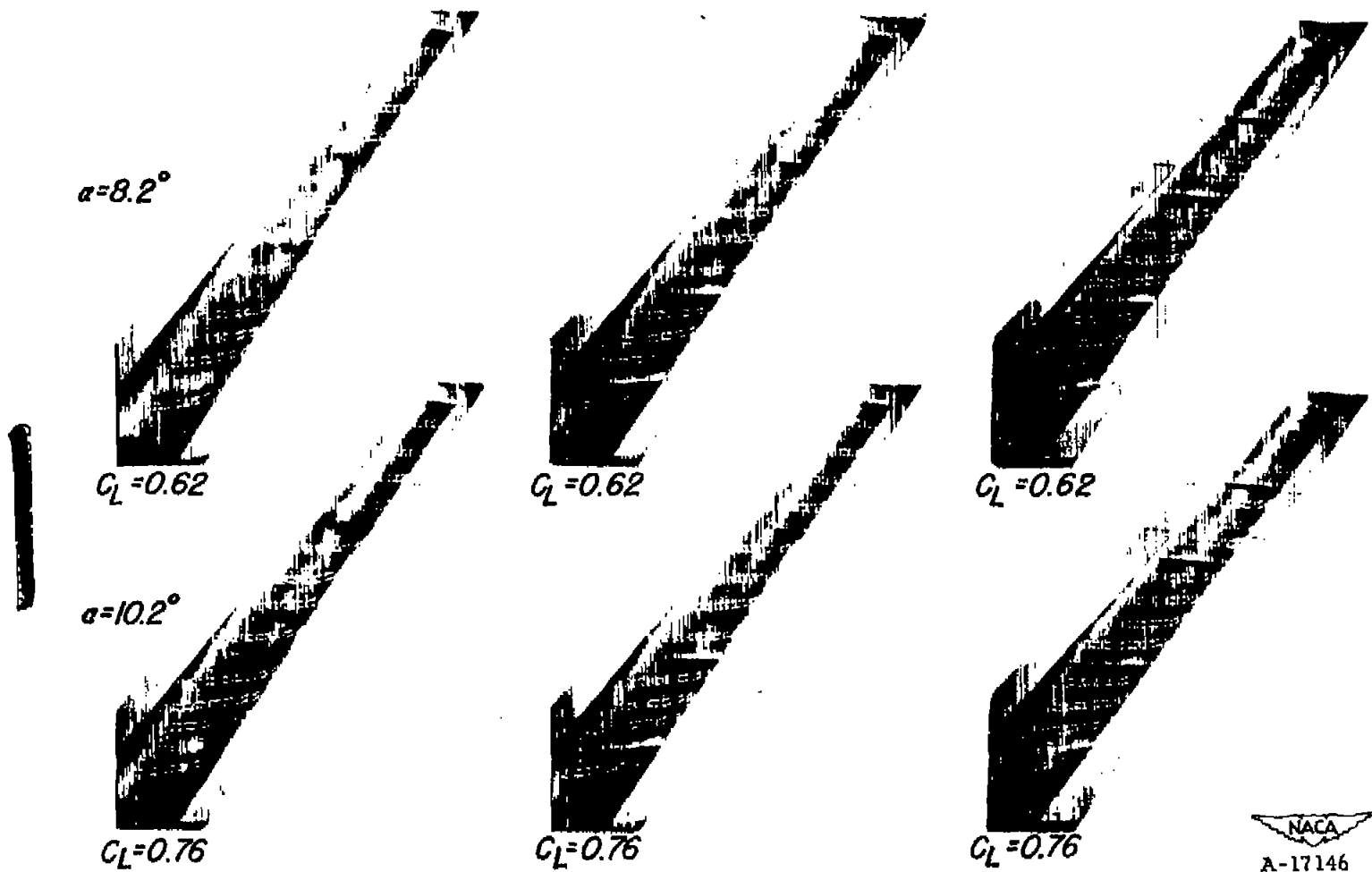
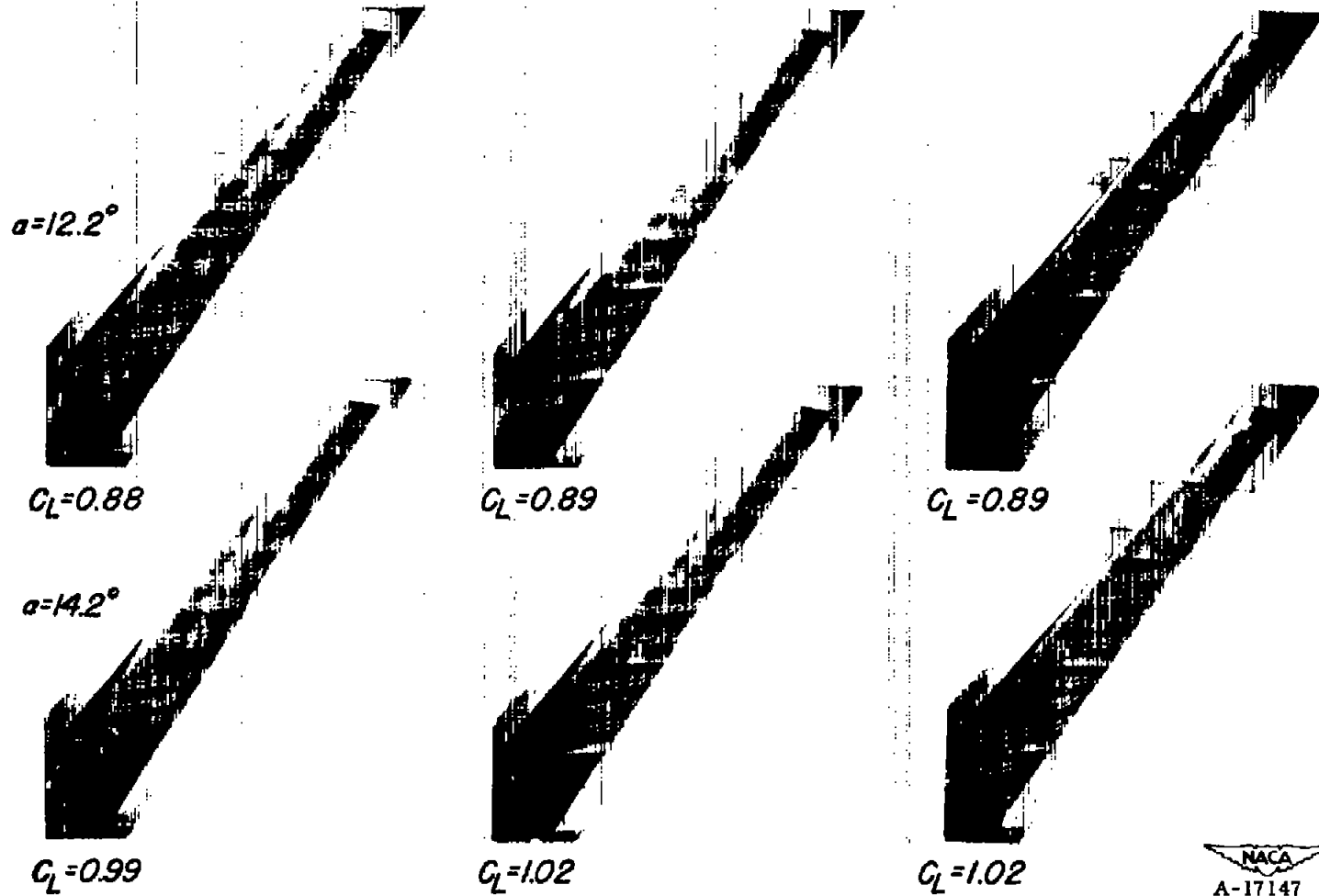


Figure 17.— The effect of four fences (one small fence at $\eta = 0.33$ and extended fences at $\eta = 0.50$, 0.70 , and 0.85) on the variation of the drag of the wing due to lift. $M = 0.165$, $R = 8,000,000$.

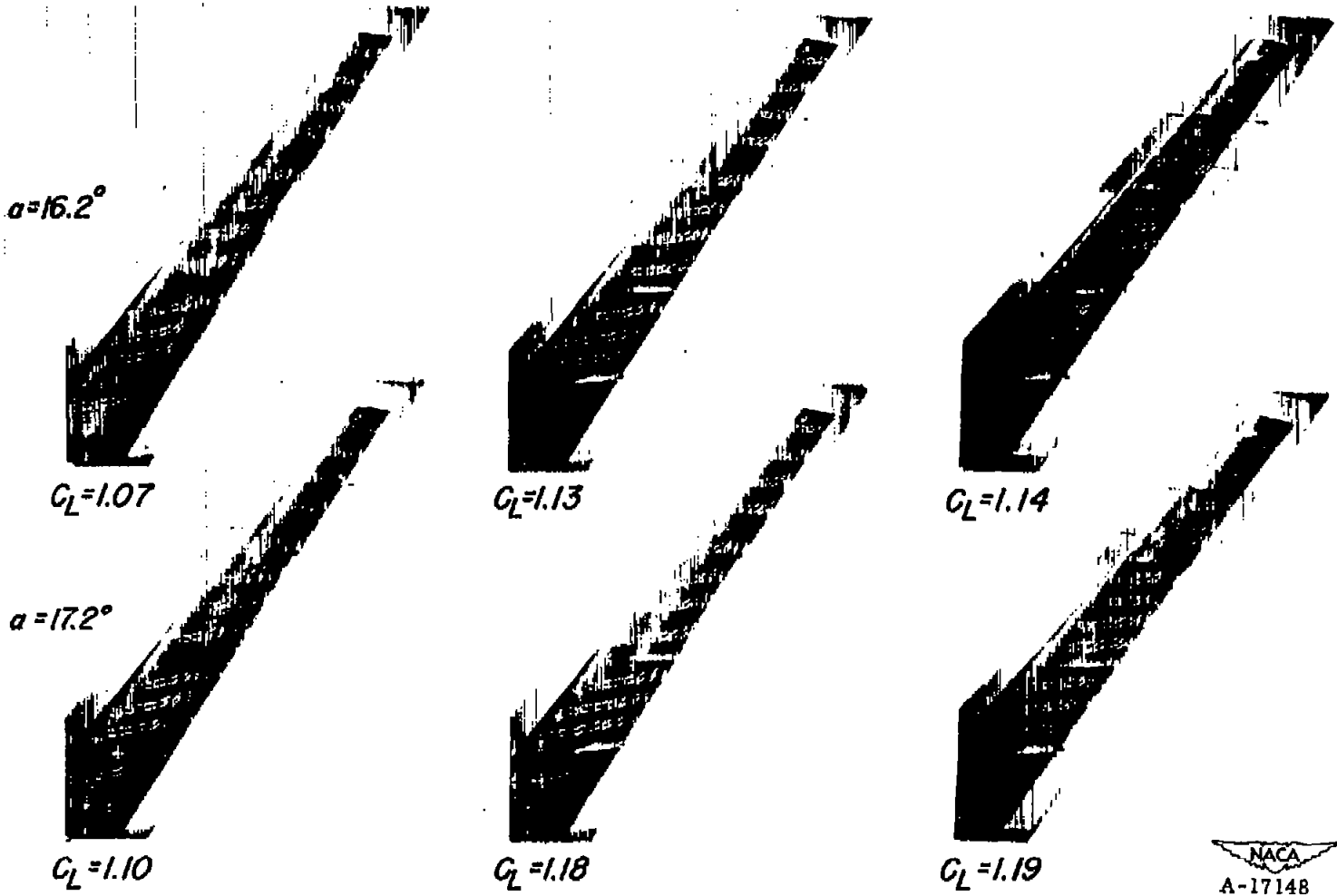


(a) $M=0.25, R=8,000,000$

Figure 18.— Photographs of tufts on the wing without fences, with three fences, and with four fences.

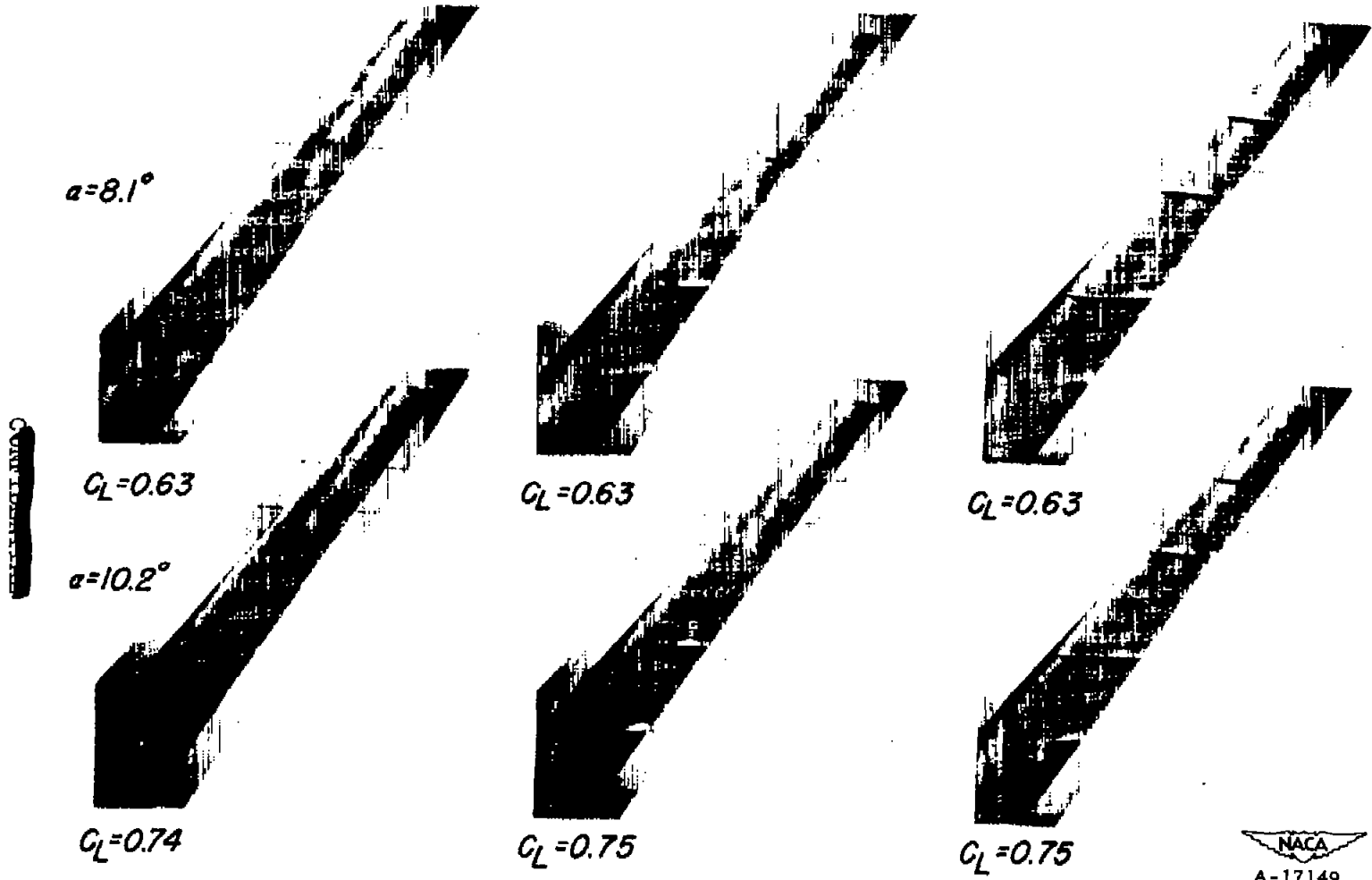


(a) Continued. $M=0.25$, $R=8,000,000$
Figure 18.—Continued.



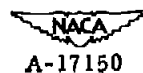
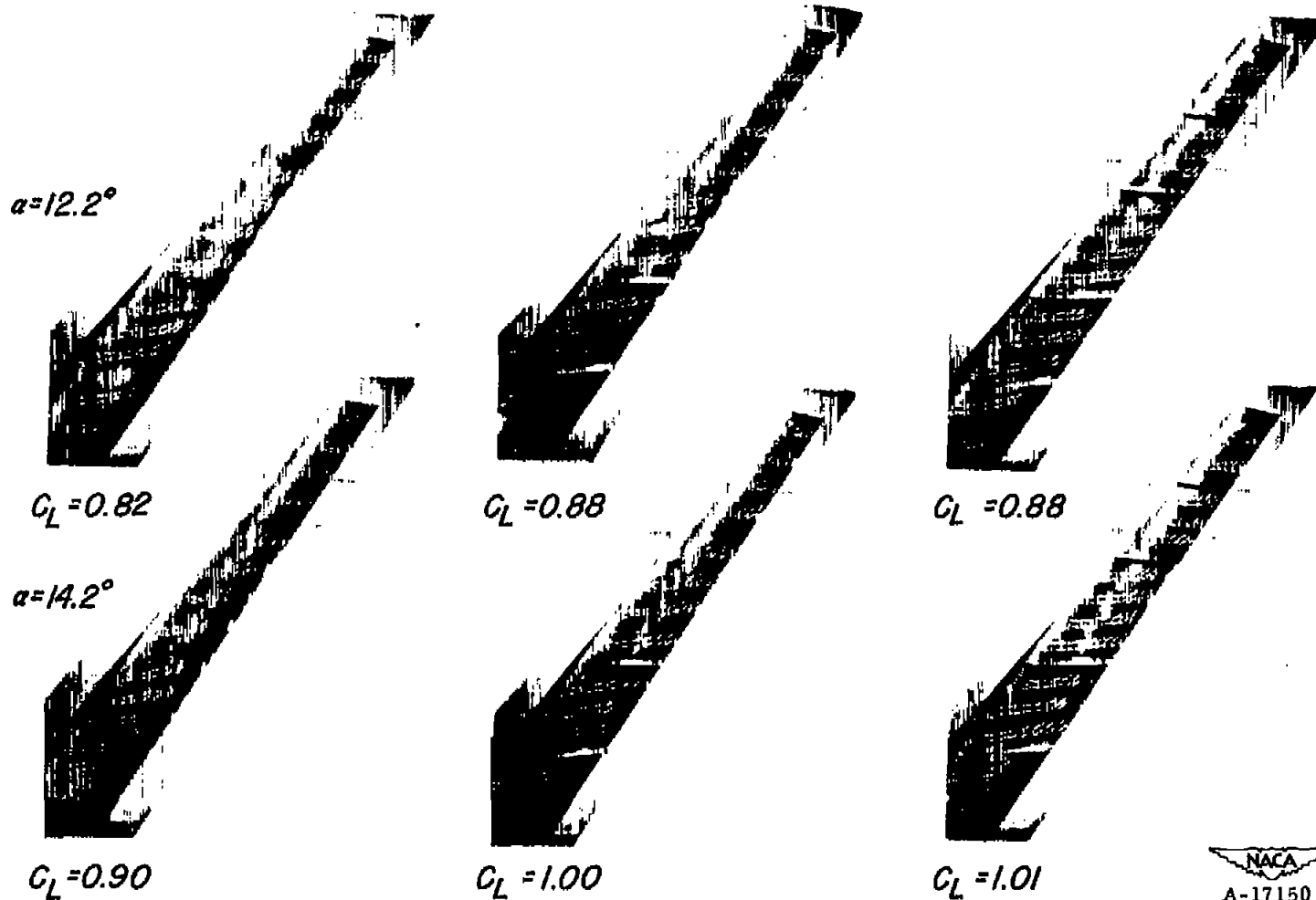
NACA
 A-17148

(a) Concluded. $M=0.25$, $R=8,000,000$
 Figure 18.—Continued.

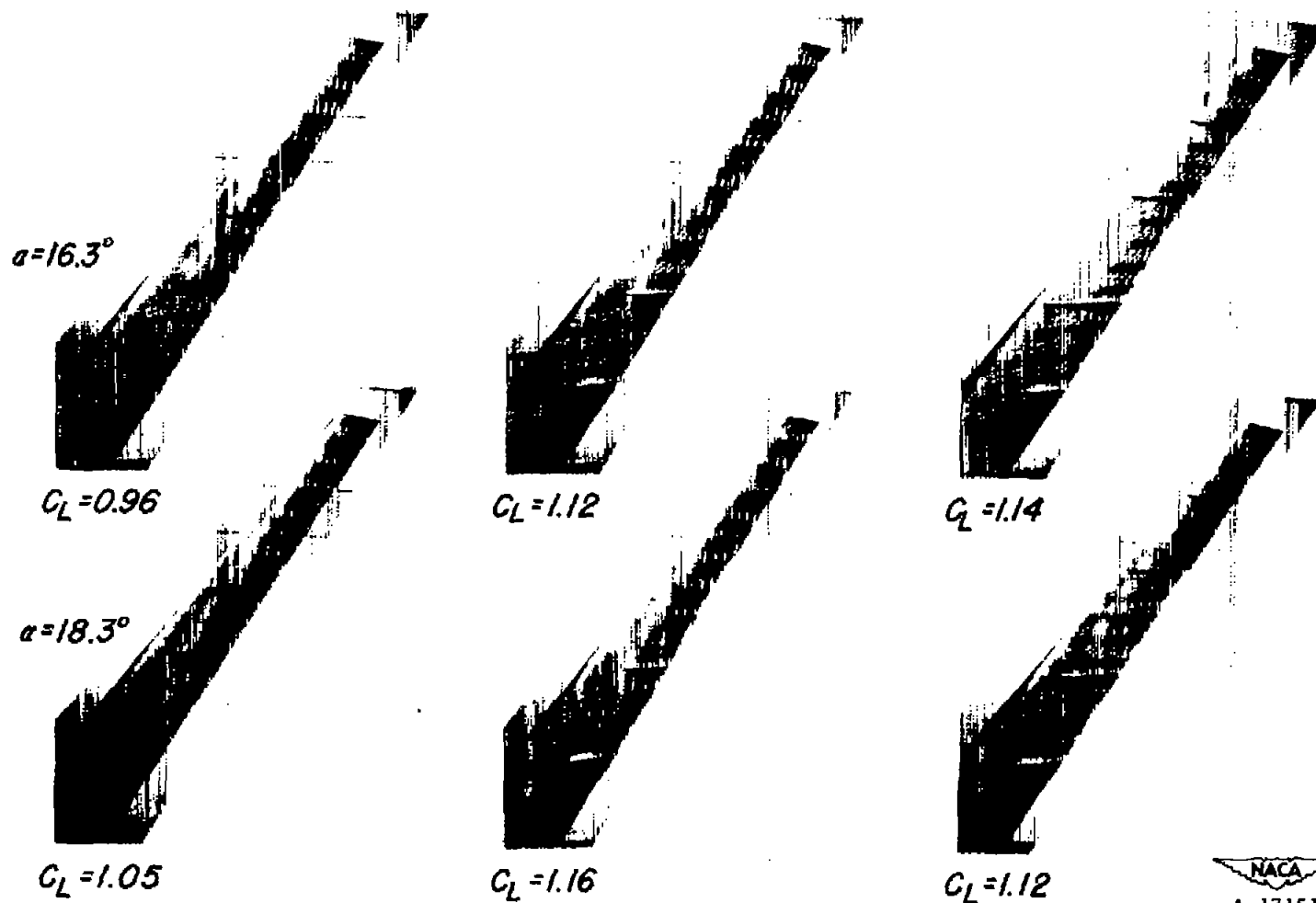


(b) $M=0.25, R=2,000,000$
Figure 18.-Continued.

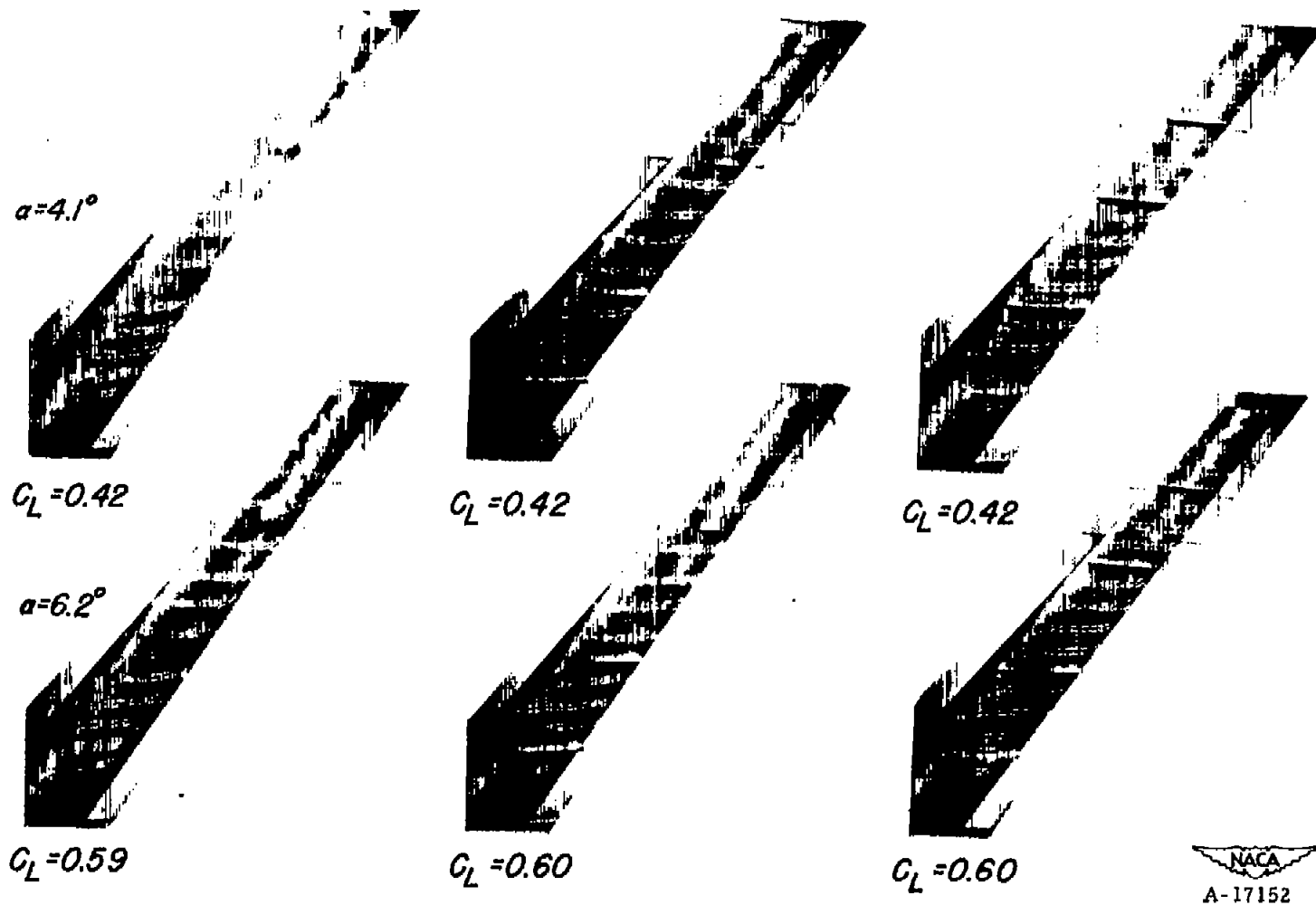
NACA
A-17149



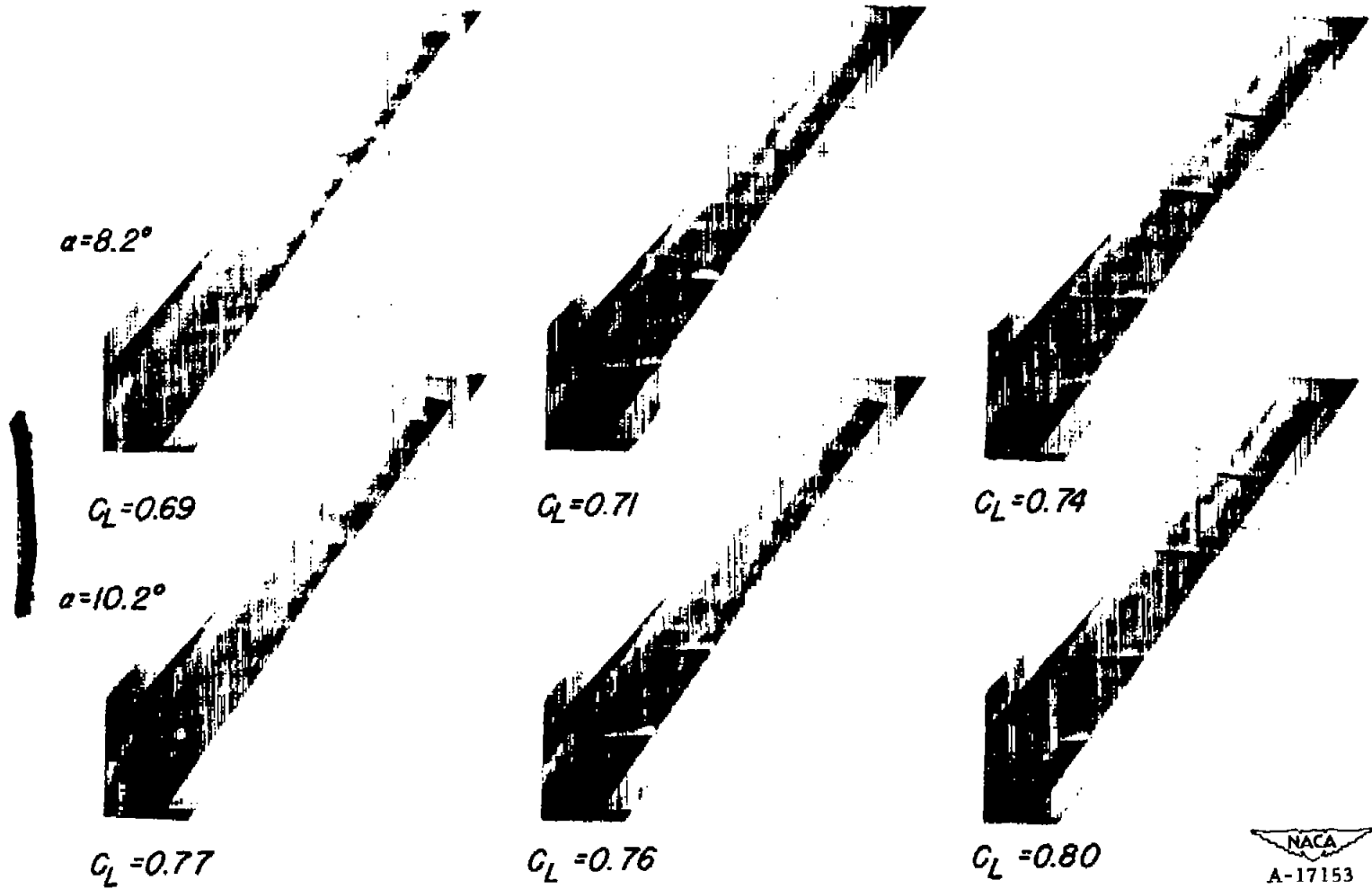
(b) Continued. $M=0.25, R=2,000,000$
 Figure 18.— Continued.



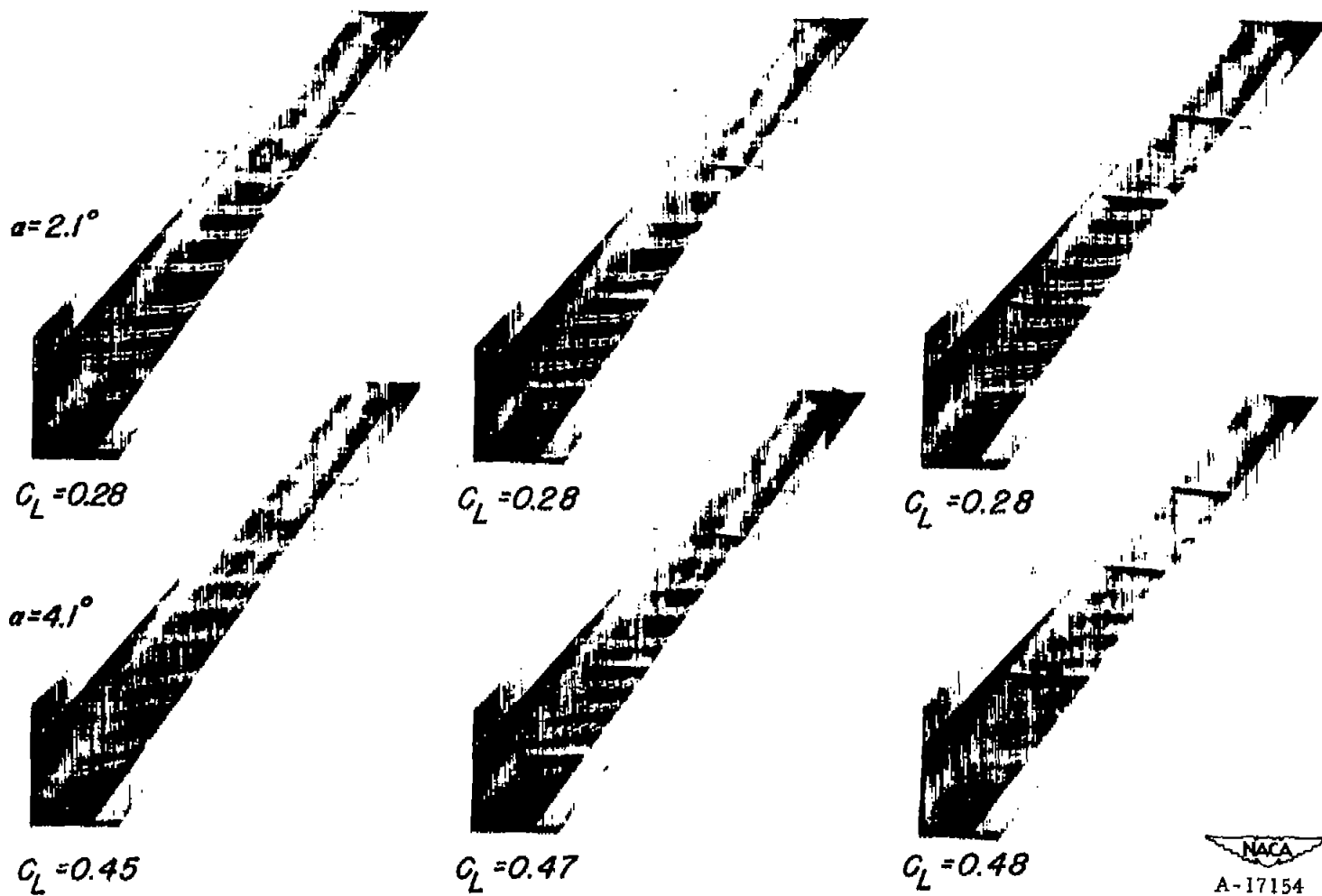
(b) Concluded. $M=0.25, R=2,000,000$
Figure 18.— Continued.



(c) $M=0.80$, $R=2,000,000$
Figure 18.—Continued.



(c) Concluded. $M=0.80, R=2,000,000$
Figure 18.—Continued.



(d) $M=0.90$, $R=2,000,000$
Figure 18.—Continued.

NACA
A-17154

$\alpha = 6.2^\circ$ $C_L = 0.56$ $\alpha = 8.2^\circ$ $C_L = 0.67$ $C_L = 0.59$ $C_L = 0.67$ $C_L = 0.62$ $C_L = 0.72$


 A-17155

(d) Concluded. $M=0.90$, $R=2,000,000$
 Figure 18. — Concluded.

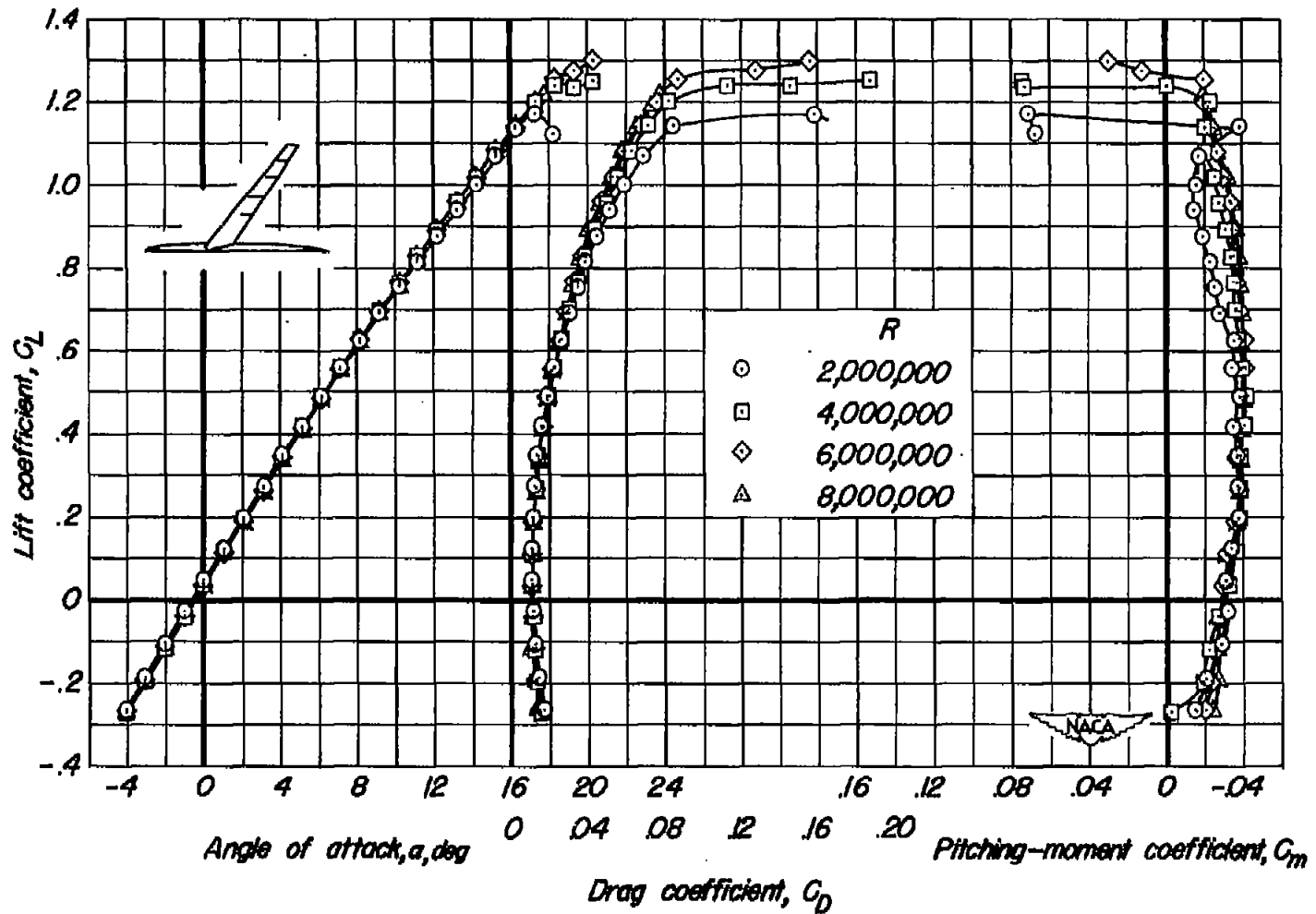


Figure 19.— The effect of Reynolds number on the lift, drag, and pitching-moment coefficients of the wing-fuselage combination with four fences. $M=0.25$.

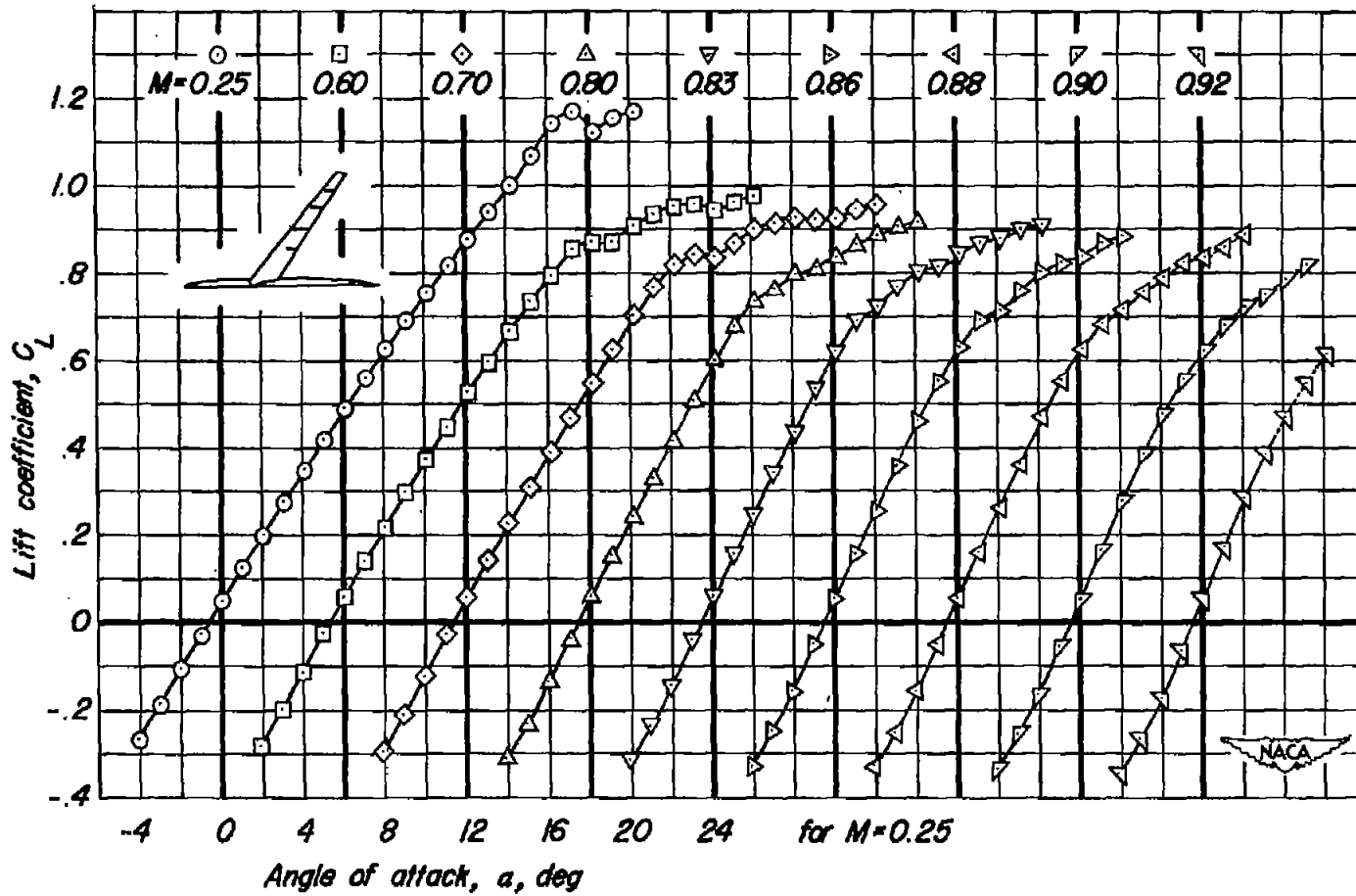
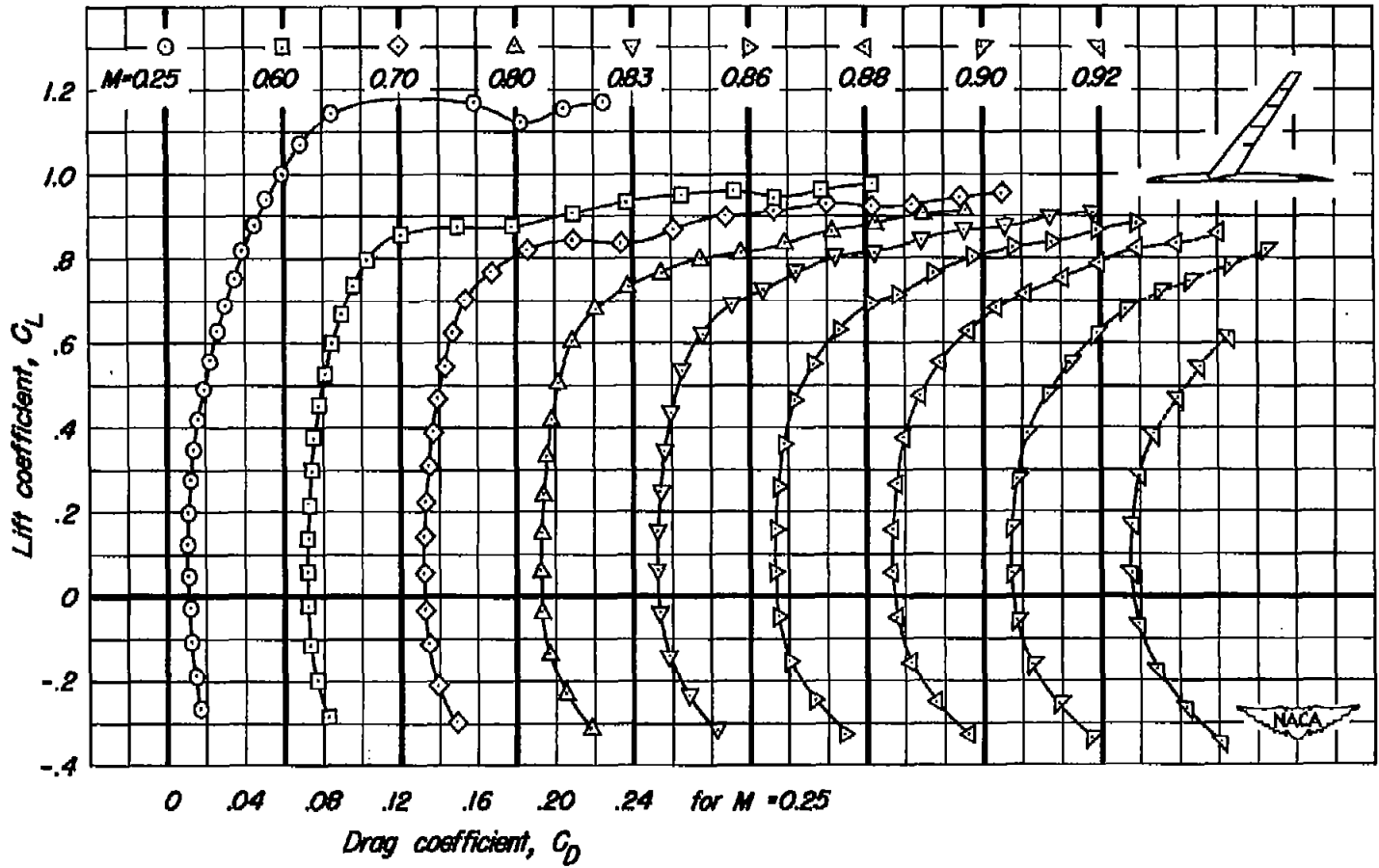
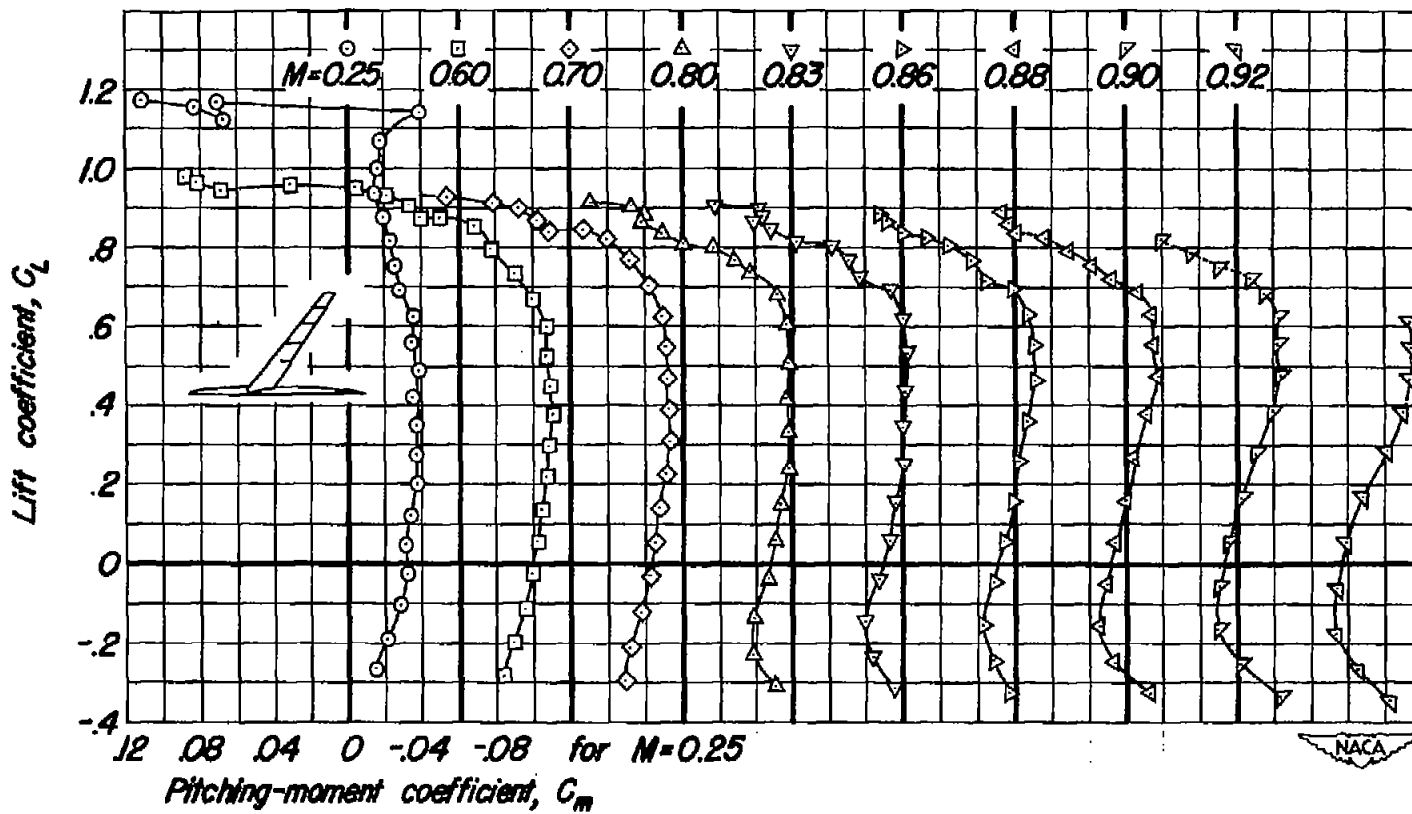
(a) C_L vs a

Figure 20.- The effect of Mach number on the lift, drag, and pitching-moment coefficients of the wing-fuselage combination with four fences. $R=2,000,000$.



(b) C_L vs C_D
 Figure 20.- Continued.



(c) C_L vs C_m
 Figure 20.- Concluded.

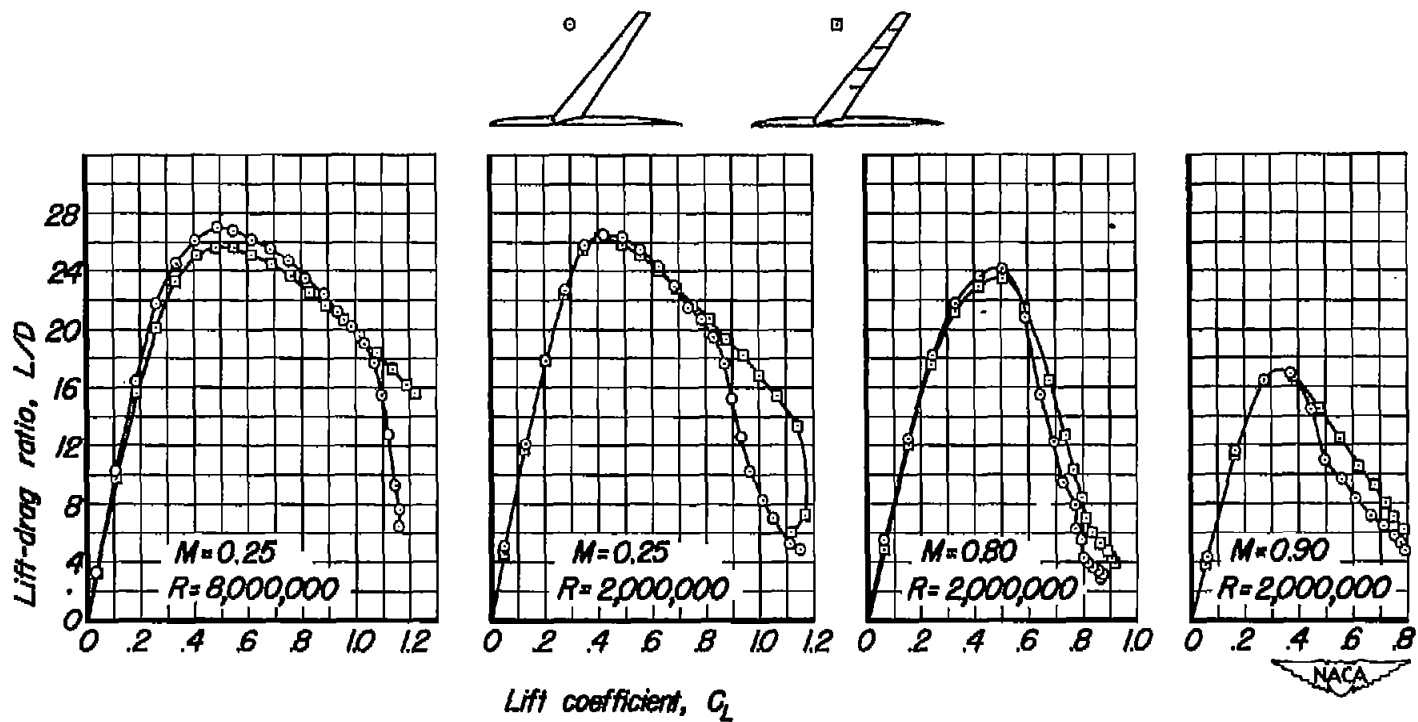


Figure 21.—The effect of four fences on the lift-drag ratio of the wing-fuselage combination.

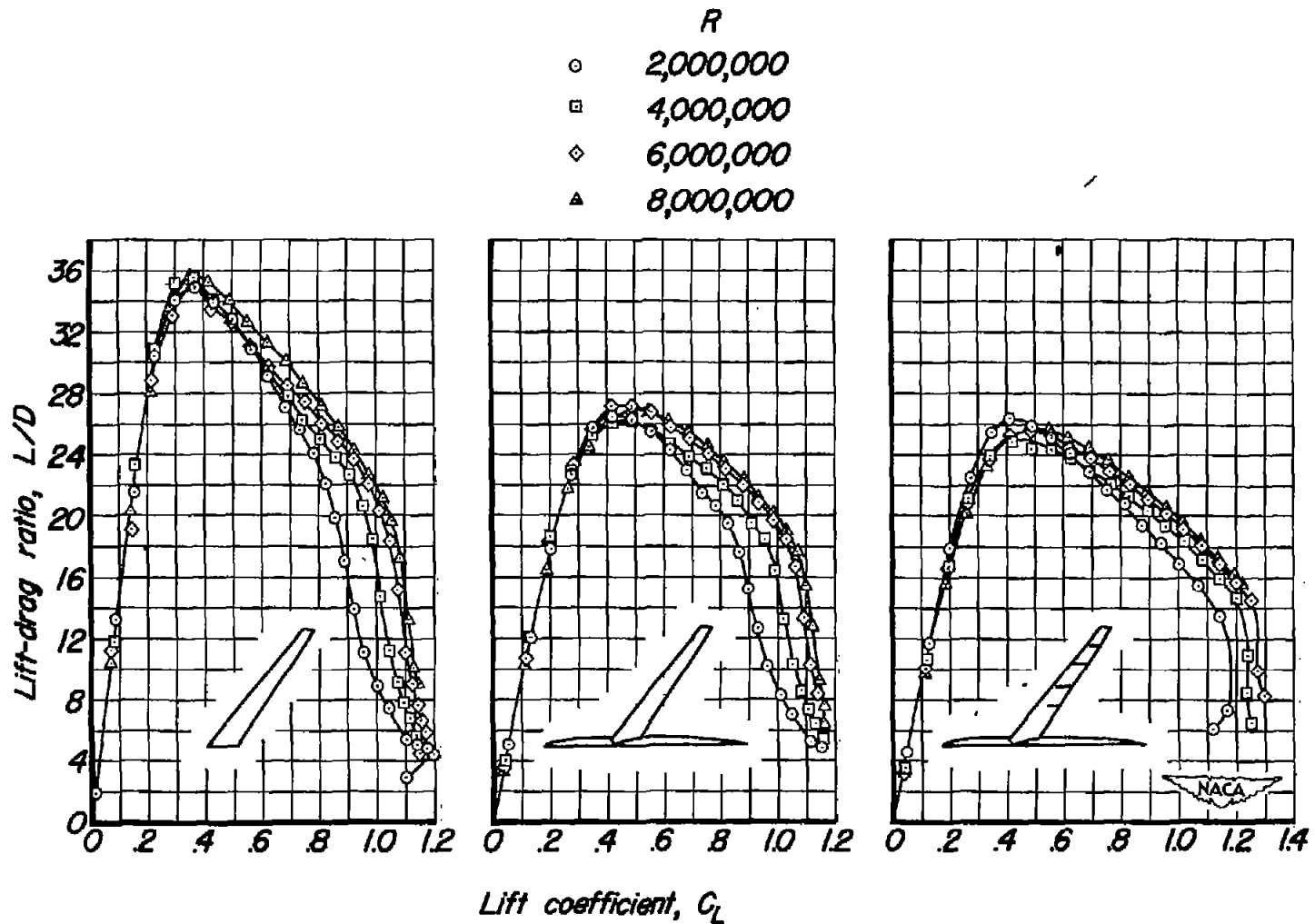
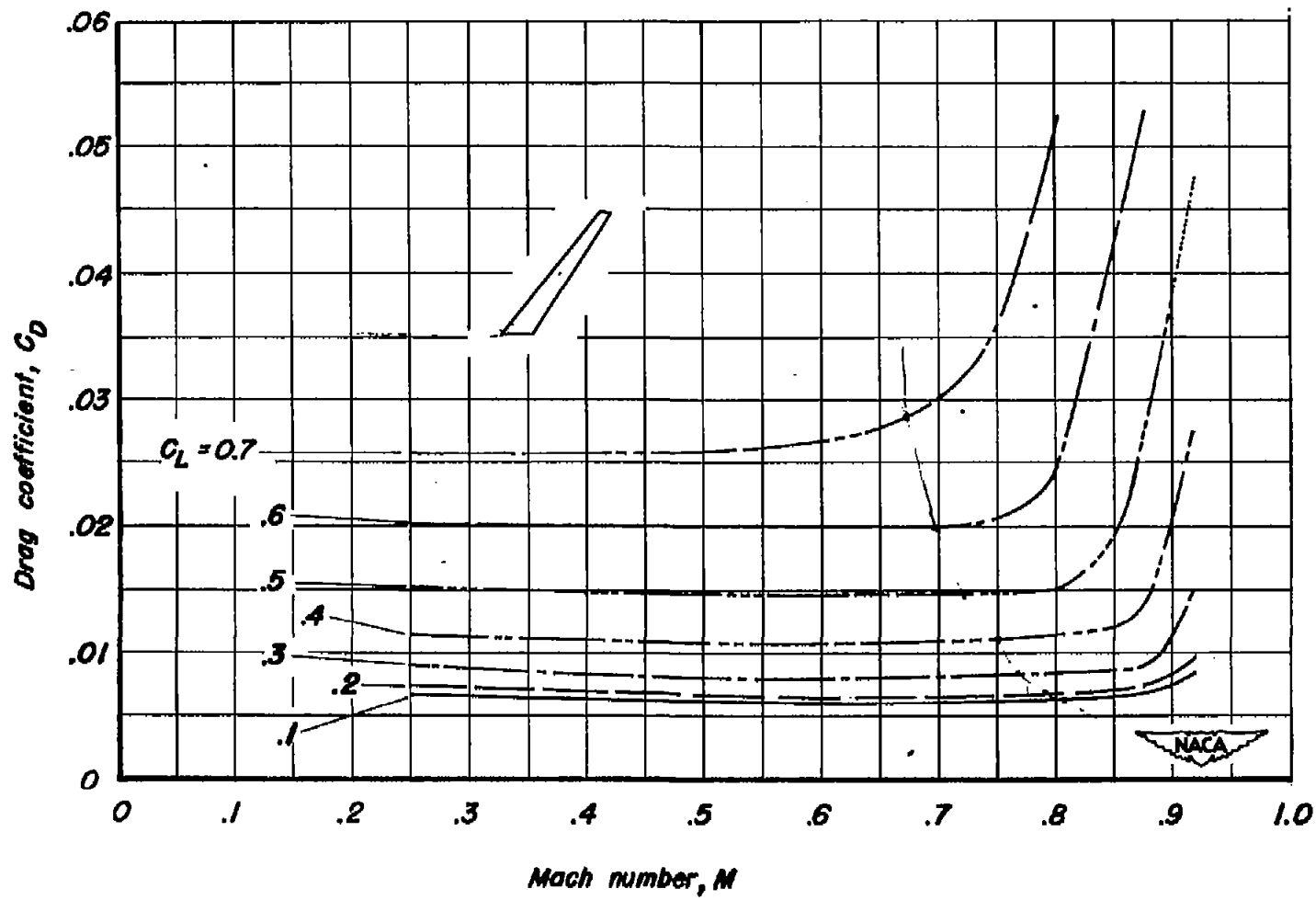
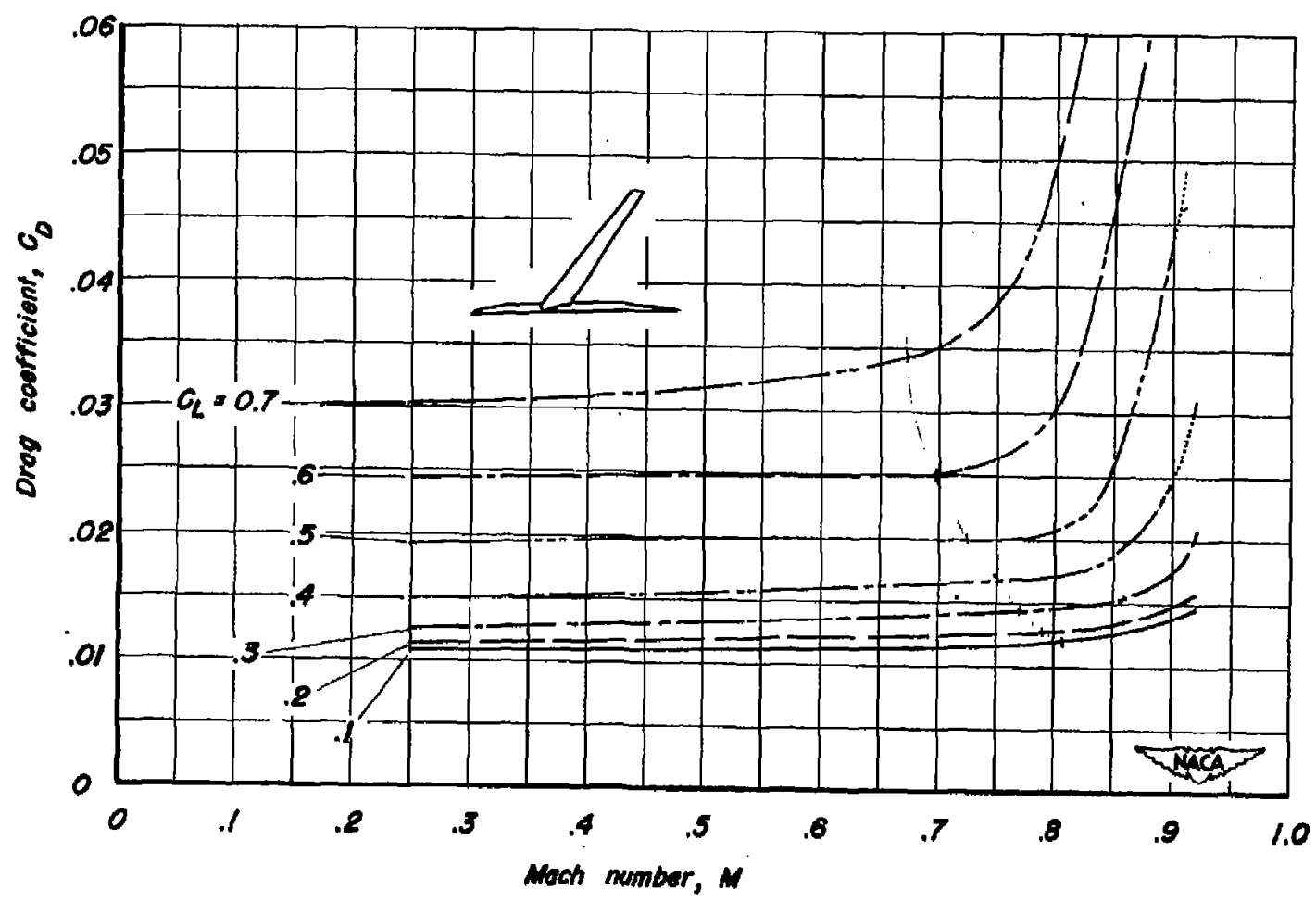


Figure 22.— The effect of Reynolds number on the lift-drag ratio. $M = 0.25$.



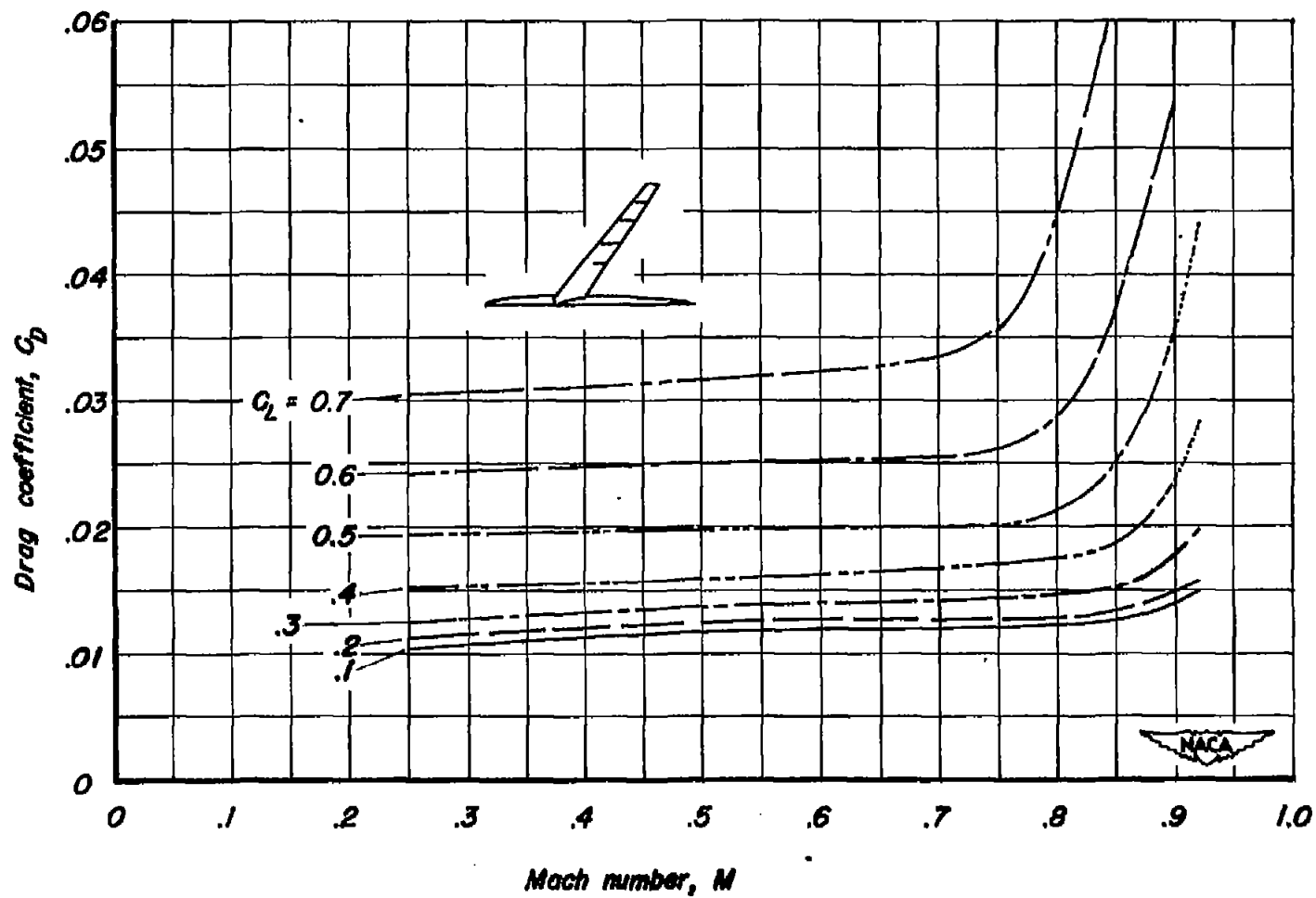
(a) Wing alone.

Figure 23.— The variation of drag coefficient with Mach number. $R=2,000,000$.



(b) Wing-fuselage combination
Figure 23.- Continued.

CONFIDENTIAL



(c) Wing-fuselage combination with four fences
Figure 23.—Concluded.

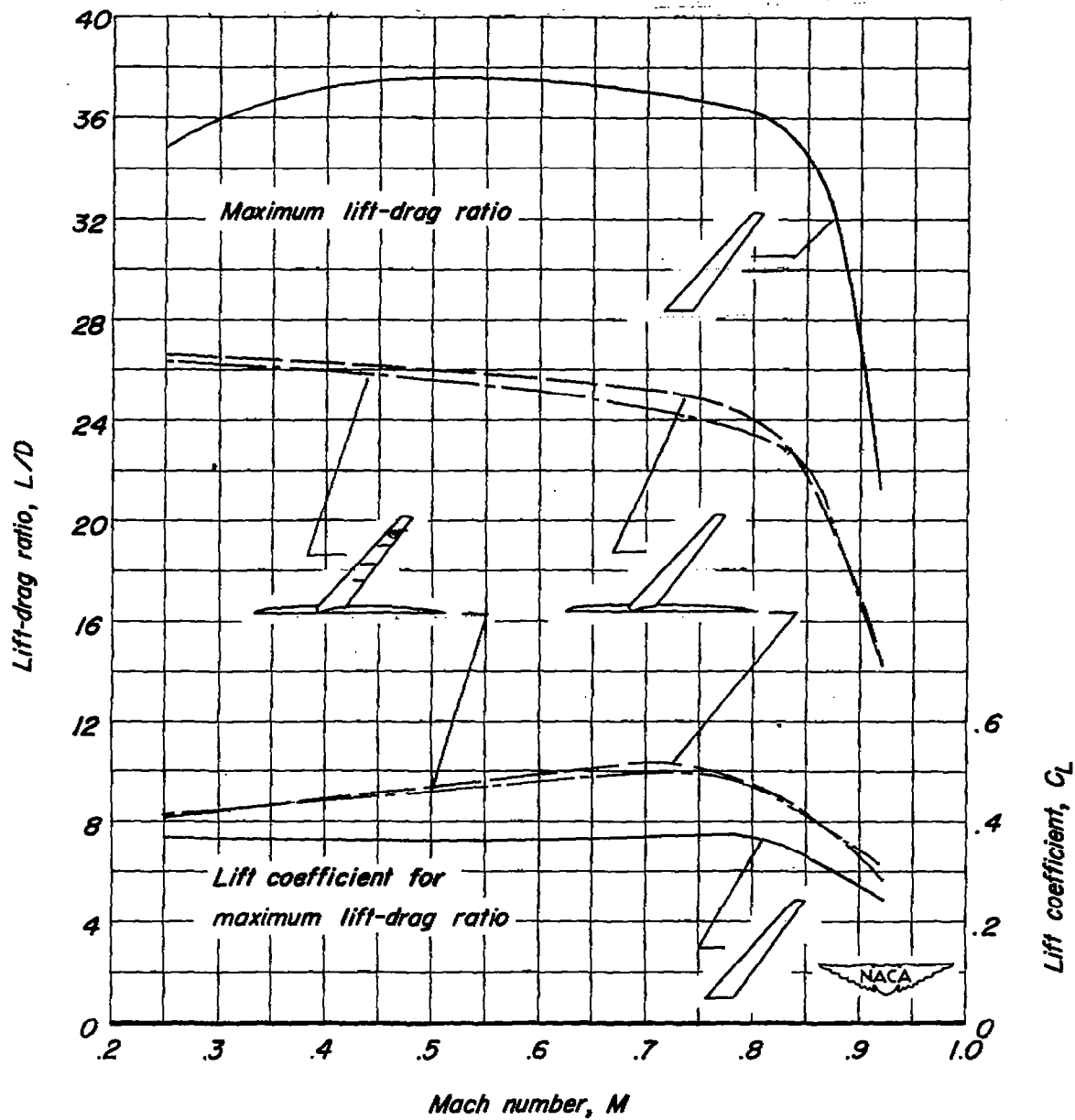


Figure 24.— The effect of Mach number on the maximum lift-drag ratio and the lift coefficient for maximum lift-drag ratio. $R=2,000,000$.

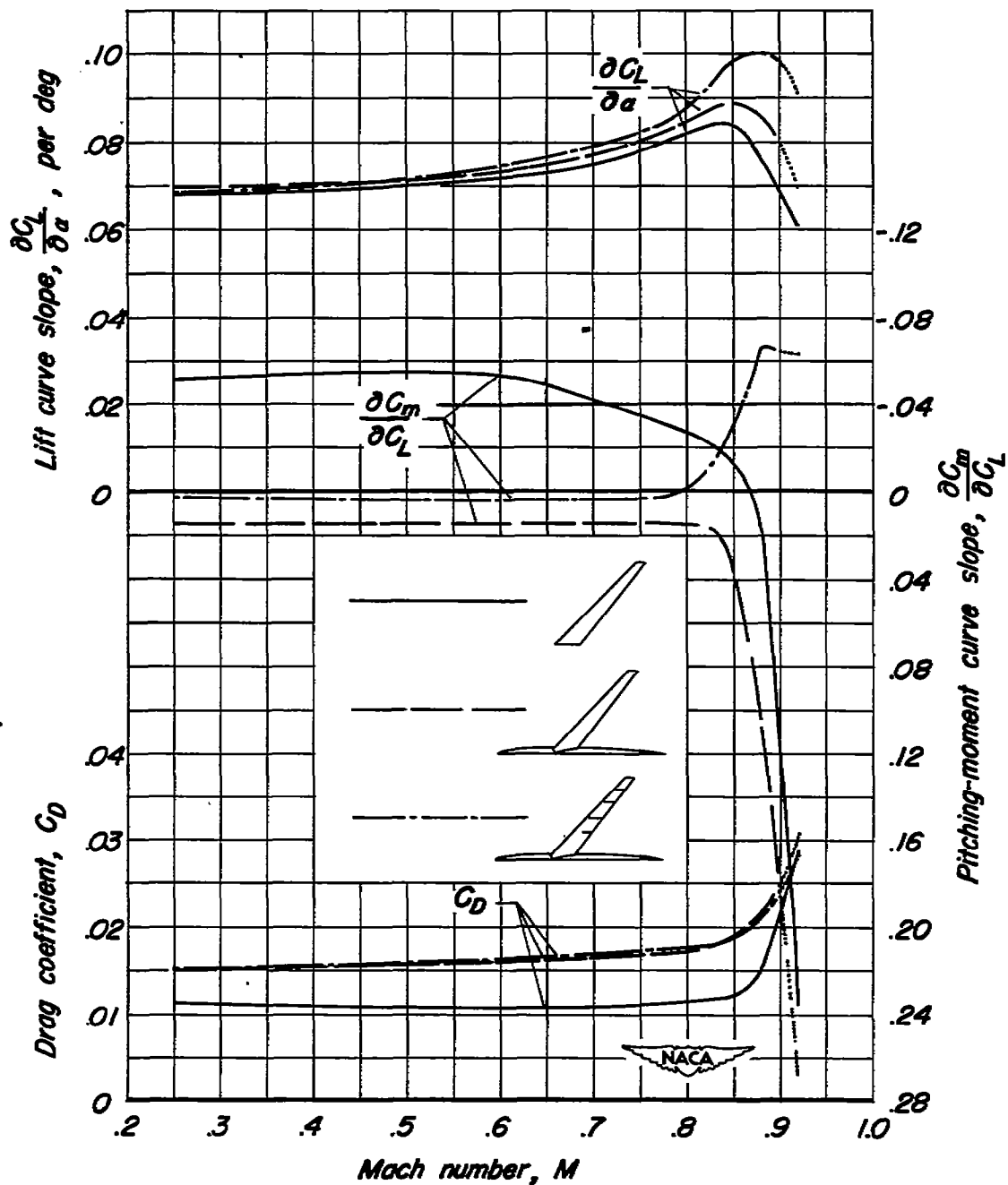


Figure 25.— The effect of Mach number on the drag coefficient, lift-curve slope and pitching-moment-curve slope. $C_L=0.4, R=2,000,000$.

SECURITY INFORMATION



3 1176 01434 8214

~~CONFIDENTIAL~~

~~CONFIDENTIAL~~